Light Gas Separations with MOFs via Predictive Modeling and Tuned Synthesis

Tina M. Nenoff
Senior Scientist
Physical, Chemical and Nano Sciences Center
Sandia National Laboratories, Albuquerque NM USA

GA Tech
March 23, 2017

Sandia Project Team

Materials:
Synthesis and Crystallography: Dorina F. Sava Gallis, Mark A. Rodriguez
DFT and AIMD: Marie V. Parkes, Jeffery A. Greathouse
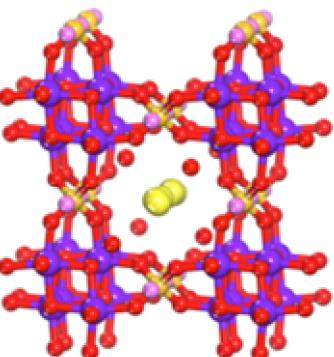Synchrotron, PDF (APS/ANL*): Karena W. Chapman

Combustion Burner Design, Build, Testing:
Chris Shaddix, Tim Williams

Techno-economic Analysis:
Scott Paap, Brandon Heimer

Novel SNL Separations and Waste Forms: Technologies for Environment and Energy Applications

R&D100 1996
JACerS, 2009, *92(9)*, 2144
JACerS, 2011, *94(9)*, 3053
*Solvent Extr. & Ion Exch*, 2012, *30*, 33

CST, Cs⁺ removal from water to Pollucite Waste Form
US Patents *6,479,427; 6,110,378*

Ag-MOR I₂(g) capture & mechanisms

JACS, 2010, *132*(26), 8897
J Phys Chem Lett, 2011, *2*,2742
I&ECR 2017, *56*(8), 2331

Fundamental Research to Applied to Commercial Products
Design the Separation Material To Develop the Waste Form

SOMS, Sr²⁺ getter, 1-step to Perovksite WF
JACS, 2002,*124(3)*, 1704
US Patent *7,122,164*

I₂/ZIF-8, Isolation to Waste Form
JACS, 2011,*133(32)*,12398
US Patent filed 2012
JACS 2013, *135*, 16256

MOFs,White Light PL
JACS, 2012,*134*(9), 3983
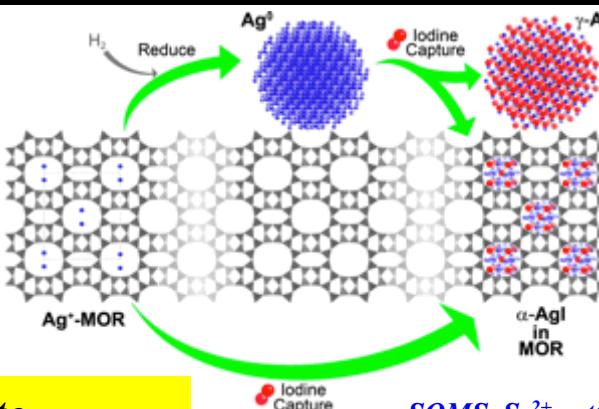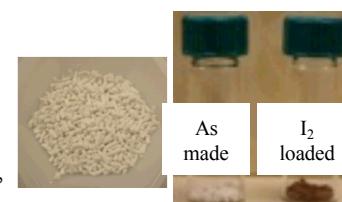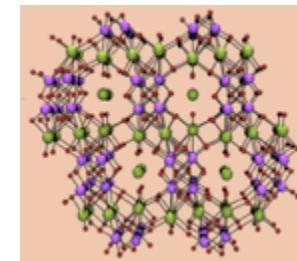*Chem Mater*, 2014, *26* (9), 2943
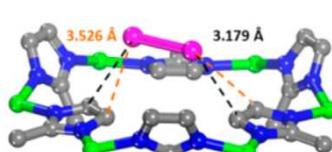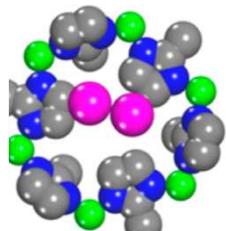
MOF Amorphization for Gas Storage
JACS, 2011,*133*(46),18583
US Patent 9,552,897; 2017
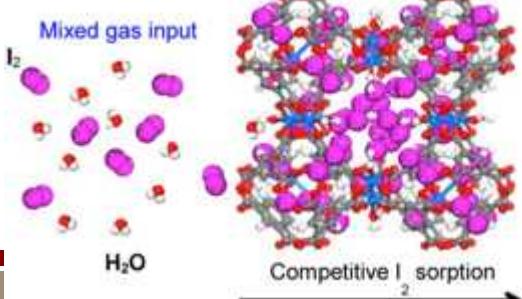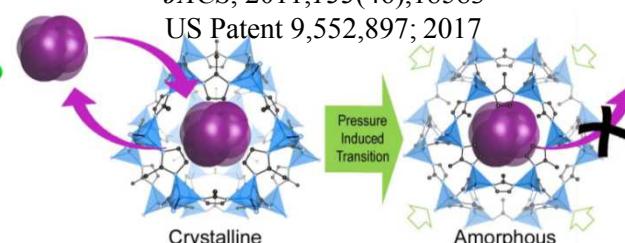
Cu-BTC: I₂from Humid Gas Stream
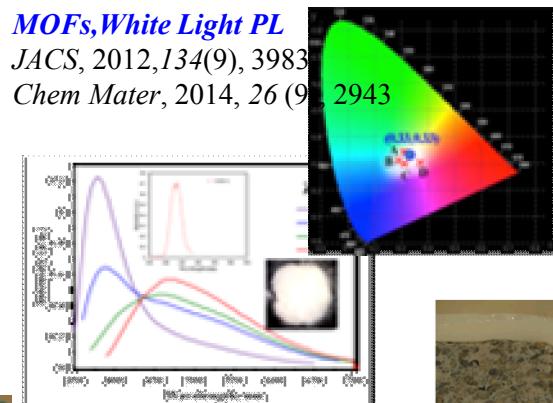*Chem. Mater*. 2013, *25*(13), 2591

As made   I₂ loaded

Binder Free MOF Pelletization
US Patent 2015
9,117,560

Universal Core-Shell Iodine Glass Waste Form & Getter
JACerS, 2011, *94*(8), 2412
US Patent 8,262,950; 2012

T. M. Nenoff, tmnenof@sandia.gov

tmnenof@sandia.gov

O$_2$/N$_2$ air separations with MOFs to Increase the Efficiency of the *ASU*

Basic Research directed to an *Energy Efficient Process* for Oxygen purification from air. *aka*: how to increase the efficiency of the air separations unit (ASU)?
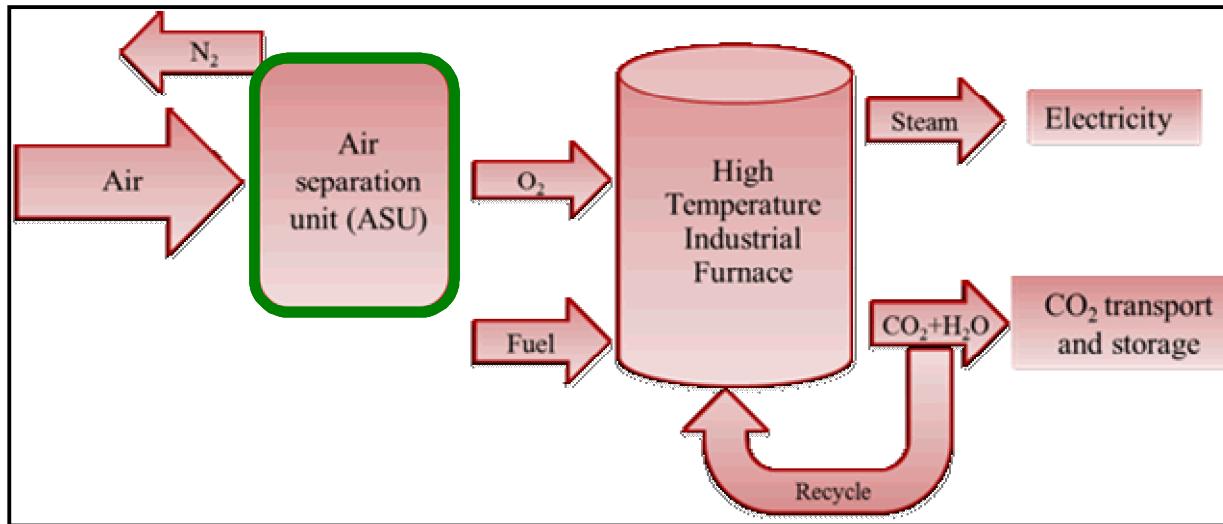
- Oxygen-enriched (oxy-fuel) combustion: burning the fossil fuel in an O$_2$ rich atmosphere results in a flue gas composed mainly of CO$_2$ and water (little or no SO$_X$ and NO$_X$ emissions)
- The limiting factor of this technology is the efficiency of the cryogenic ASU, a costly and energy intensive process (primarily compression)
- Our study is focused on new highly selective materials (MOFs) to increase the efficiency of this separation process
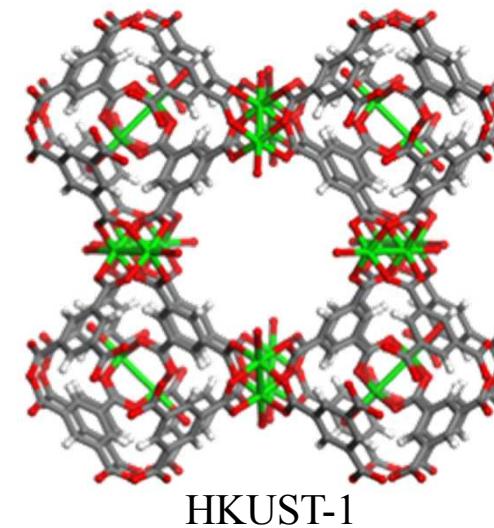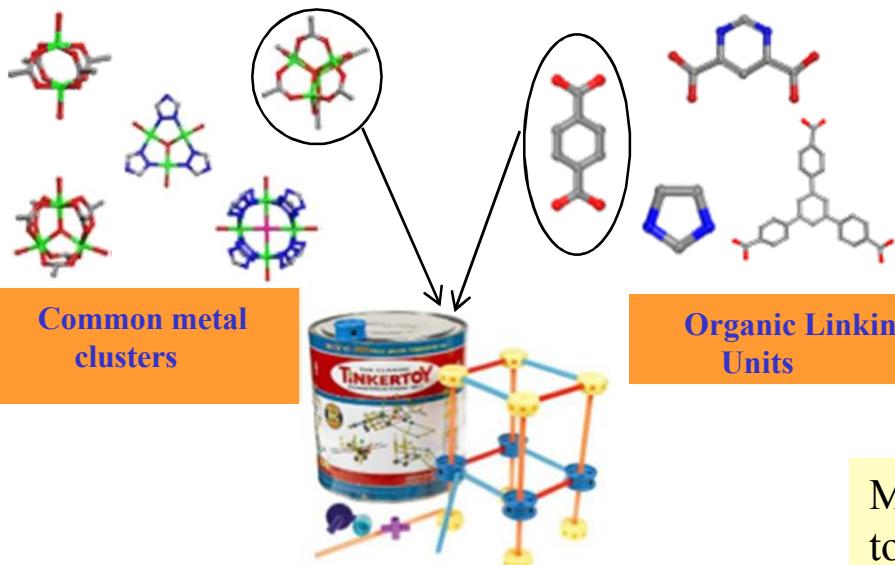
tmnenof@sandia.gov

Air Separations Materials in place of Cryogenic Separations

Zeolites
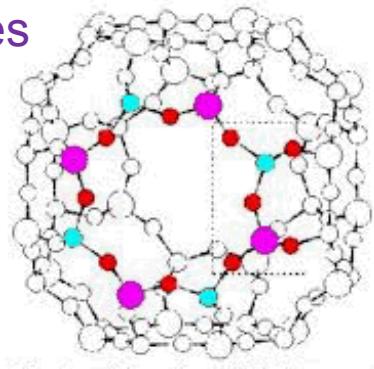
Traditionally Zeolite A is used to separate N_2 from air allowing air components to flow through: O_2, CO_2, Ar

This results in a < 90% O_2 purity product stream

MOFs

Common metal clusters

Organic Linking Units

HKUST-1

MOFs: Target high oxygen selectivity frameworks to produce > 95% O_2 purity

tmnenof@sandia.gov

DFT Simulations Provide Molecular-level Details
Metal-O_2 and Metal-N_2 Binding Energies and Geometries

- MOFs with coordinatively unsaturated metal centers are promising materials for O_2/N_2 separations

- Two prototypical MOFs from this category, $Cr_2(BTC)_3$ (*JACS* **2010**, *132*, 7856–7857) $Fe_2(DOBDC)$ (*JACS* **2011,** *133*, 14814-14822) both show preferential adsorption of O_2 over N_2

- Plane wave DFT calculations were performed on periodic structures in the Vienna Ab initio Simulation Package (VASP)

- Binding geometries for side-on and bent O_2 and bent and linear geometries for N_2 were evaluated

- Static binding energies for O_2 and N_2 at 0 K
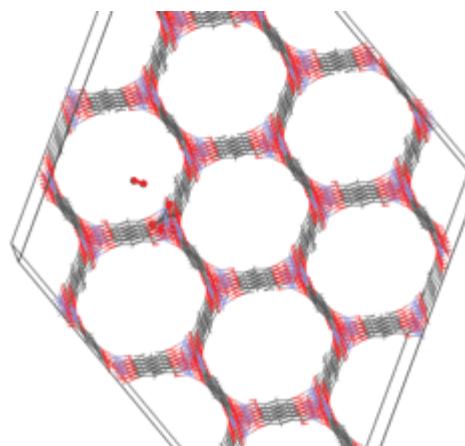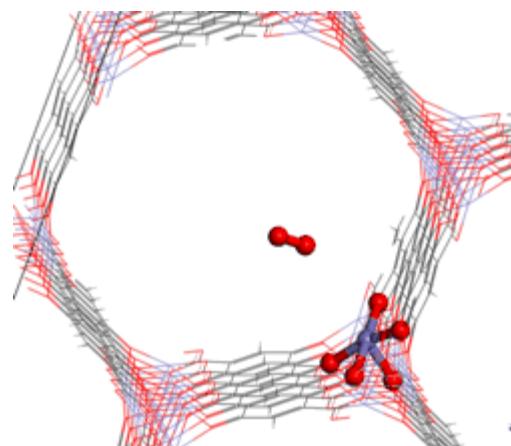
MOF with O_2 in pore O_2 ready to bind to metal O_2 bound to metal

6
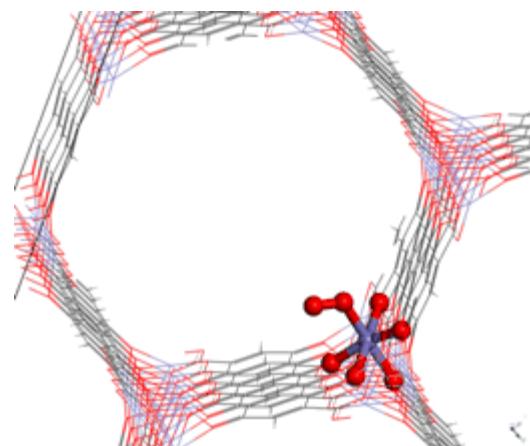
DFT modeling of of Oxygen Adsorption in Varied Metal-Centered MOFs

M$_2$(dobdc)

M$_3$(btc)$_2$
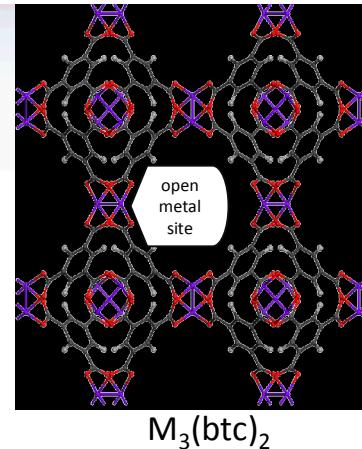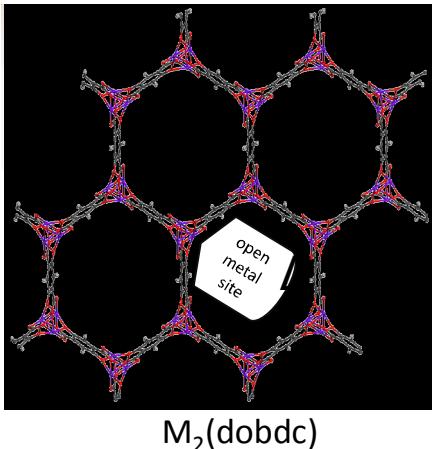
Plan wave density functional theory (DFT) calculations were performed on periodic structures of each MOF in the Vienna ab initio simulation package **(VASP)** with the Perdew-Burke-Ernzerhof **(PBE)** functional including dispersion corrections **(DFT-D2)**. Geometries were optimized and **static binding energies (ΔE_{O2}, ΔE_{N2})** were calculated by

$$\Delta E_{O2} = E_{MOF+O2} - E_{MOF} - E_{O2}$$

The **differences in binding energies ($\Delta\Delta E$)** for oxygen and nitrogen were calculated by
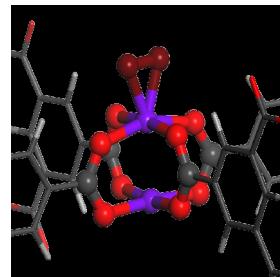
$$\Delta\Delta E = -(\Delta E_{O2} - dE_{N2})$$

MOF metal sites = separate O$_2$/N$_2$ by differences in bonding & electronic properties

Attention Paid to Bonding Geometries

Side-on bonding
∠M-X-X 67° - 71°

Cr$_3$(btc)$_2$(O$_2$)
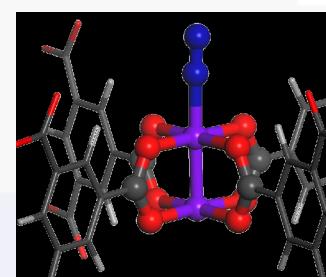
Bent bonding
∠M-X-X 116° - 159°

Mn$_2$(dobdc)(O$_2$)
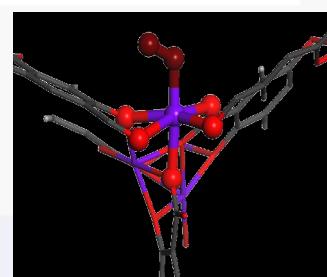
Linear bonding
∠M-X-X 165° - 179°

Fe$_3$(btc)$_2$(N$_2$)

7

O$_2$ and N$_2$ binding energies trends across the first row transition metal series

tmnenof@sandia.gov
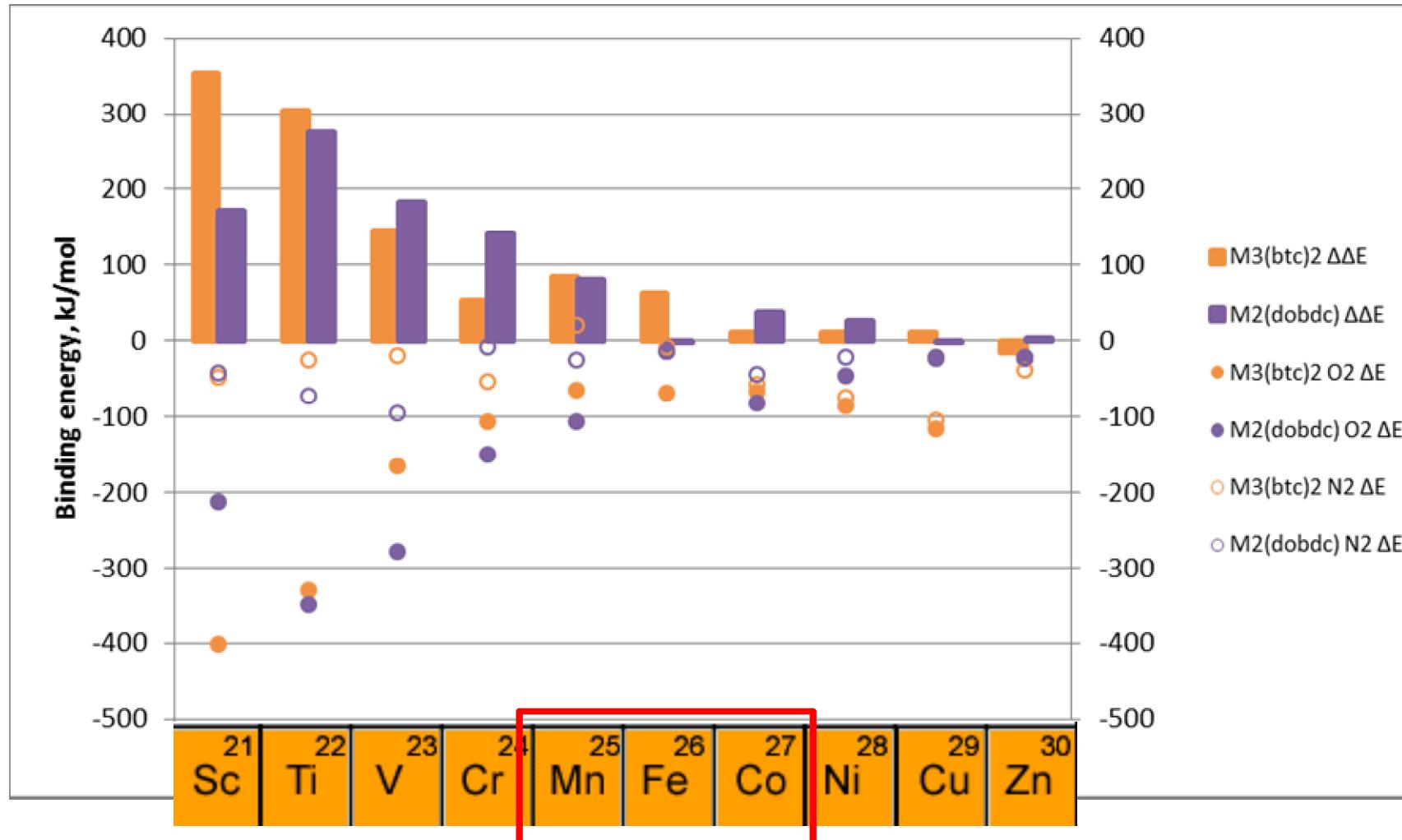
Need/Desire To Retain Porosity of MOF For Studies of Metal-O_2 Bonding Effects

• The effect of Porous analogues of Cu-BTC include: Cr, Mo, Ru, Ni (the Ru and Ni have much lower than expected surface areas, 1000-1100 m^2/g)

• Porphyrin-templated Mn-, Fe- and Co- Cu-BTC analogues known, however no measurable accessible porosity (*J. Am. Chem. Soc.* **2012**, *134*, 928−933)
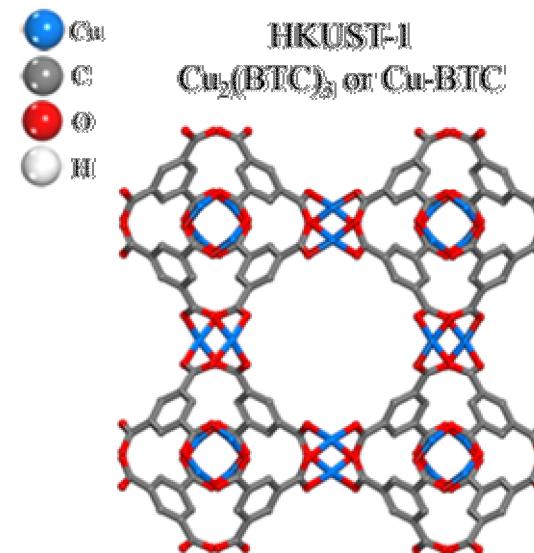
Chui, S. S. Y et.al Science **1999**, 283, 1148.

Postsynthetic metal ion exchange

Cu-BTC $\xrightarrow{MCl_2 \cdot (H_2O)_x, \ DMF, \ 90°C}$ M/Cu-BTC

M = **Mn, Fe, Co**

9

tmnenof@sandia.gov
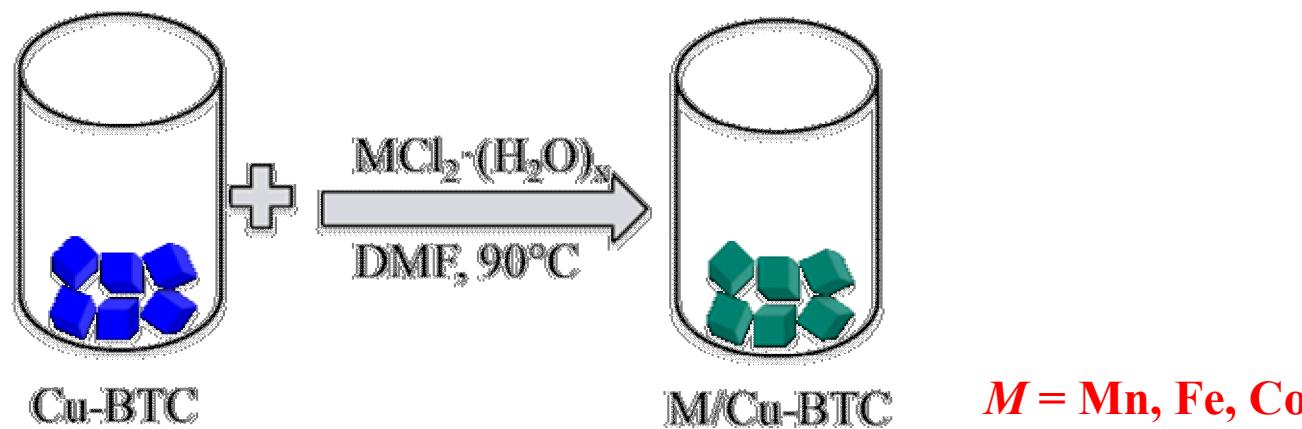
Confirmation of In-Framework Metal Substitution – Unit Cell Expansion & Elemental Mapping

XRD

- Co@Cu-BTC
- Fe@Cu-BTC
- Mn@Cu-BTC
- Cu-BTC
- simulated Cu-BTC

Intensity, a.u.

2-theta/⁰

SEM-EDS
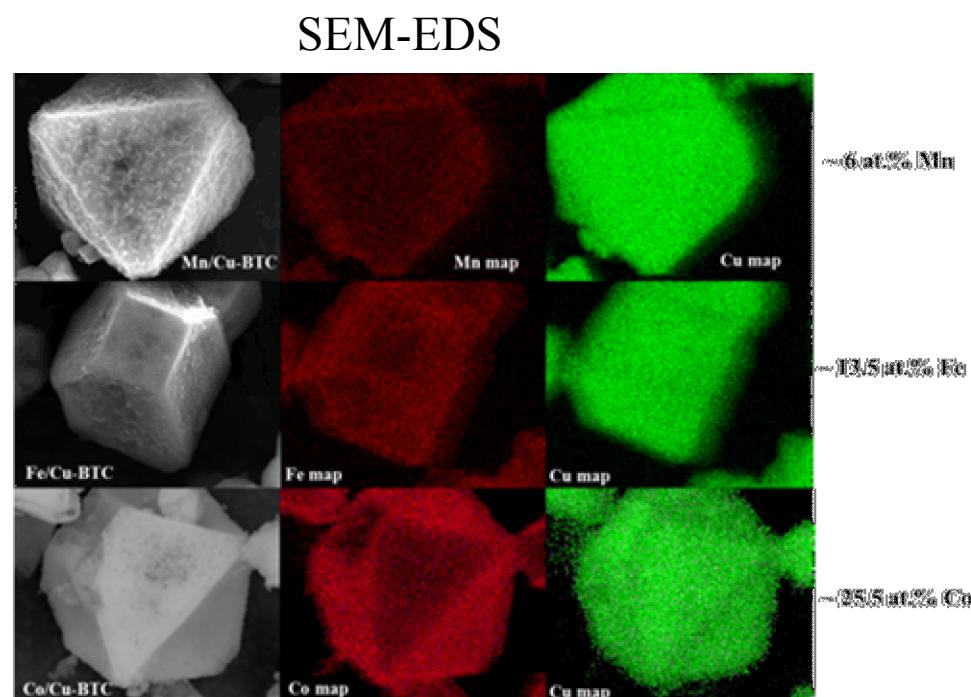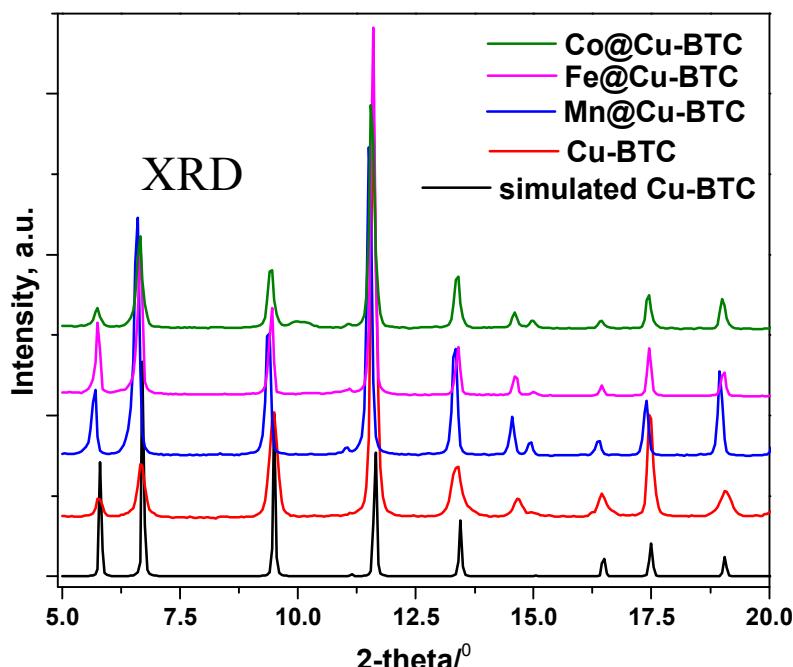
	Expansion (Å)	M-O average bond length (Å)
Cu-BTC	–	1.7
Co/Cu-BTC	0.043	2.08
Fe/Cu-BTC	0.019	2.0
Mn/Cu-BTC	0.030	2.17

Excellent DFT and Experiment Correlation at Low Temperature and Low Pressure

Cu>Mn>Fe>Co (DFT)
Cu>Mn>Fe>Co (exp)

	DFT O_2 binding energy, kJ/mol	DFT N_2 binding energy, kJ/mol
Cu-BTC	-116	-105
Mn/Cu-BTC	-113	-97
Fe/Cu-BTC	-110	-92
Co/Cu-BTC	-104	-93

For uptake at the lowest partial pressure measured (~0.01 P/P$_0$)
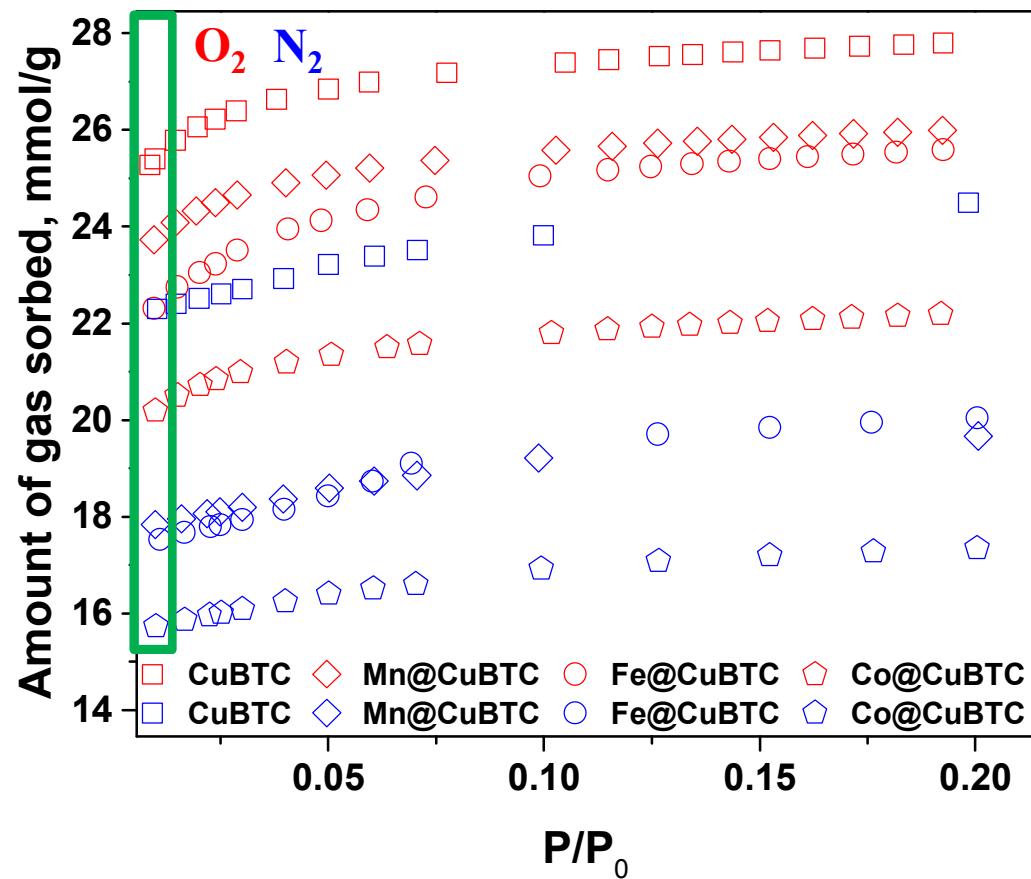
O_2 (red) and N_2 (blue) adsorption isotherms measured at 77K on pristine Cu-BTC and Mn-, Fe-, and Co-substituted samples

Isoteric Heats of Adsorption for O_2 (red) and N_2 (blue) Comparison of Cu-BTC vs Fe/Cu-BTC Data
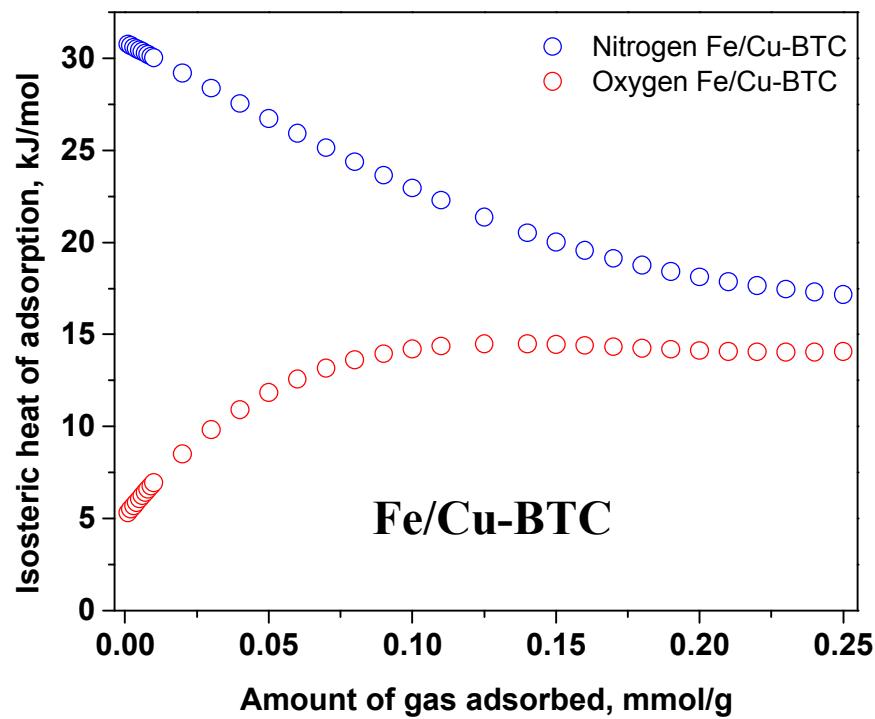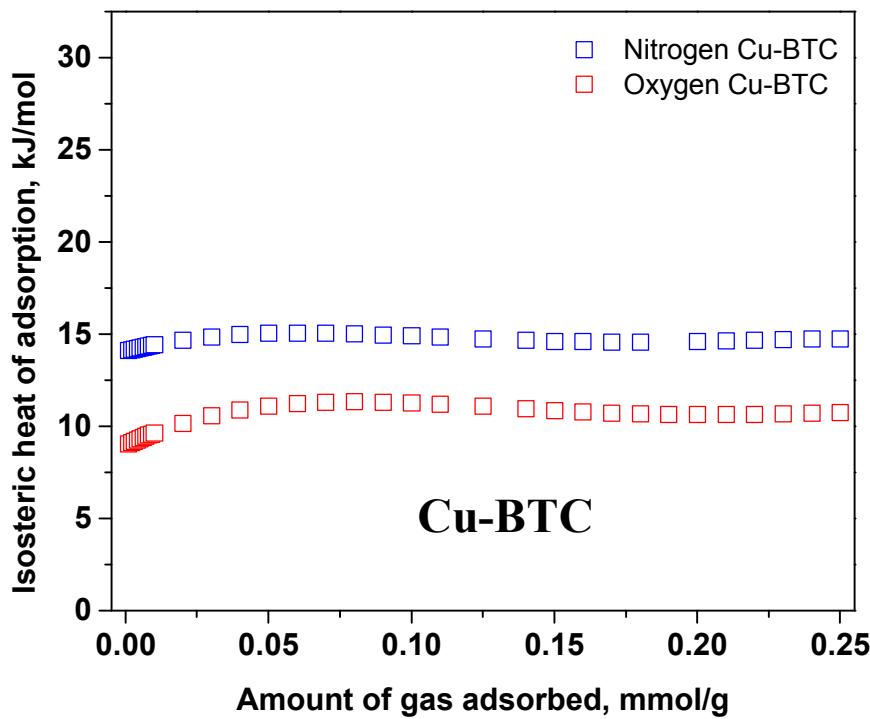
The 0 K *DFT binding energy* calculations do not correlate as well with experimental data from 273-298 K

tmnenof@sandia.gov

Use of AIMD to Predict Behavior of Dynamic Gas Molecules

Vienna *ab initio* simulation package (VASP)

- MOF
  - M_2(dobdc) analogs
- Metals

- Temperatures
  - 201 K
  - 258 K
  - 298 K

- AIMD simulations
  - NVT ensemble
  - 27.5 ps
  - 0.5 fs timestep
- PBE density functional with dispersion correction (PBE-D2), PAW potentials for core electrons, spin polarization

13

tmnenof@sandia.gov

Guests

2 O_2 bound
4 O_2 unbound

2 N_2 bound
4 N_2 unbound

Single component

Mixed gas
Competitive binding

6 N_2 bound
4 O_2 unbound

6 O_2 bound
4 N_2 unbound

Temperatures

201 K
258 K
298 K

Metals

24	25	26
Cr	Mn	Fe

Red Sky Supercomputer
36 Simulations

3,800 processor-days each

http://hpc.sandia.gov/

14
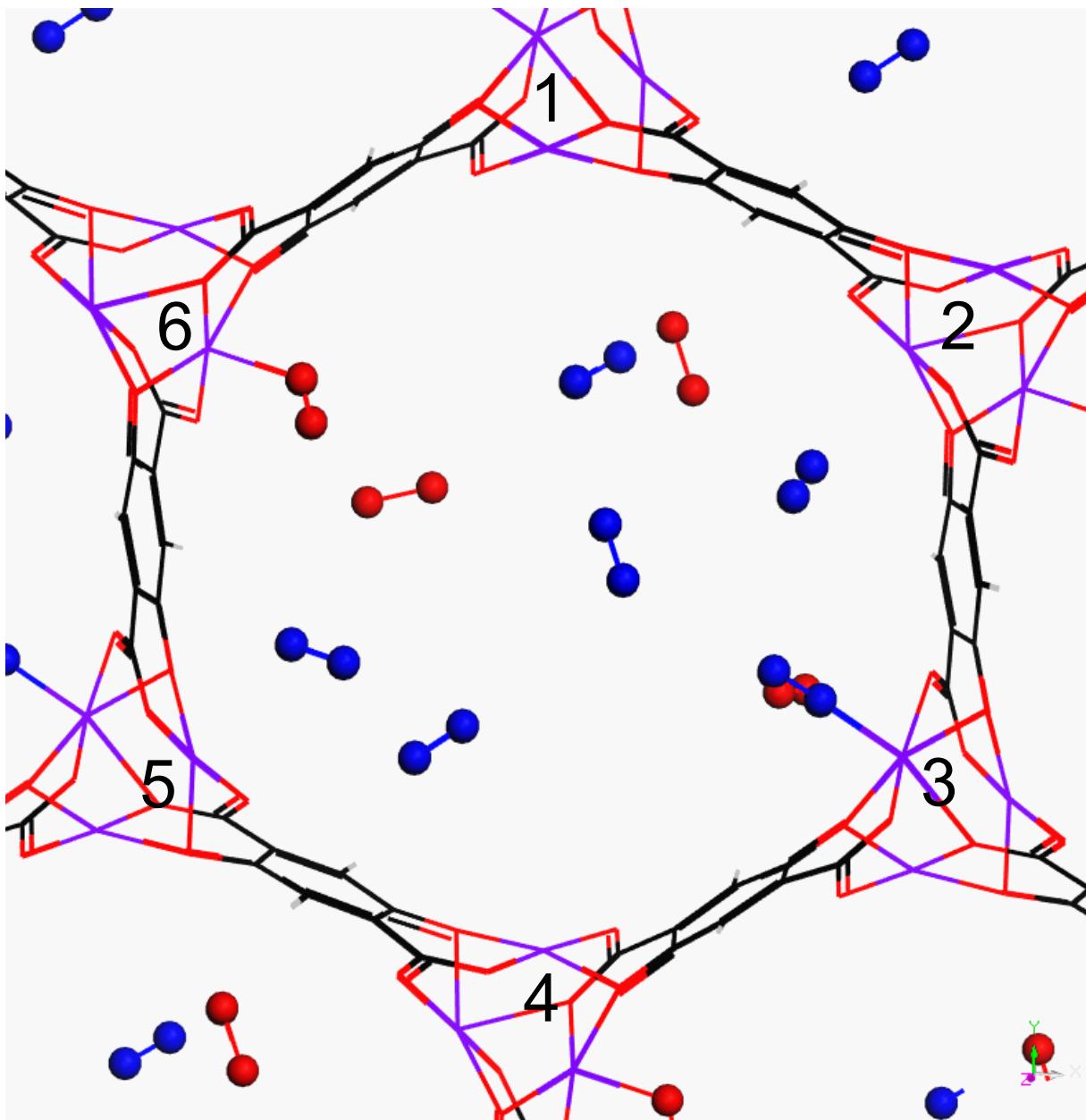
Cr$_2$(dobdc)
6 N$_2$ + 4 O$_2$
298 K

NVT
Time 2 ps – 15 ps

1 frame = 25 fs

- O$_2$ slow to bind, but once on metal center, binding holds

- N$_2$ rapid bind and release from metal centers

- O$_2$ long term binding is consistently 'bent'

- Selective for O$_2$

tmnenof@sandia.gov

Gas Occupancy at Each Metal Site

Cr$_2$(dobdc), 298 K
6 N$_2$ bound + 4 O$_2$ in pore

- O$_2$ bound bent
- O$_2$ bound side-on
- N$_2$ bound

-10 kJ/mol

-147 kJ/mol

~ Shaded section viewed in previous video

Cr #

timestep (0.5 fs)
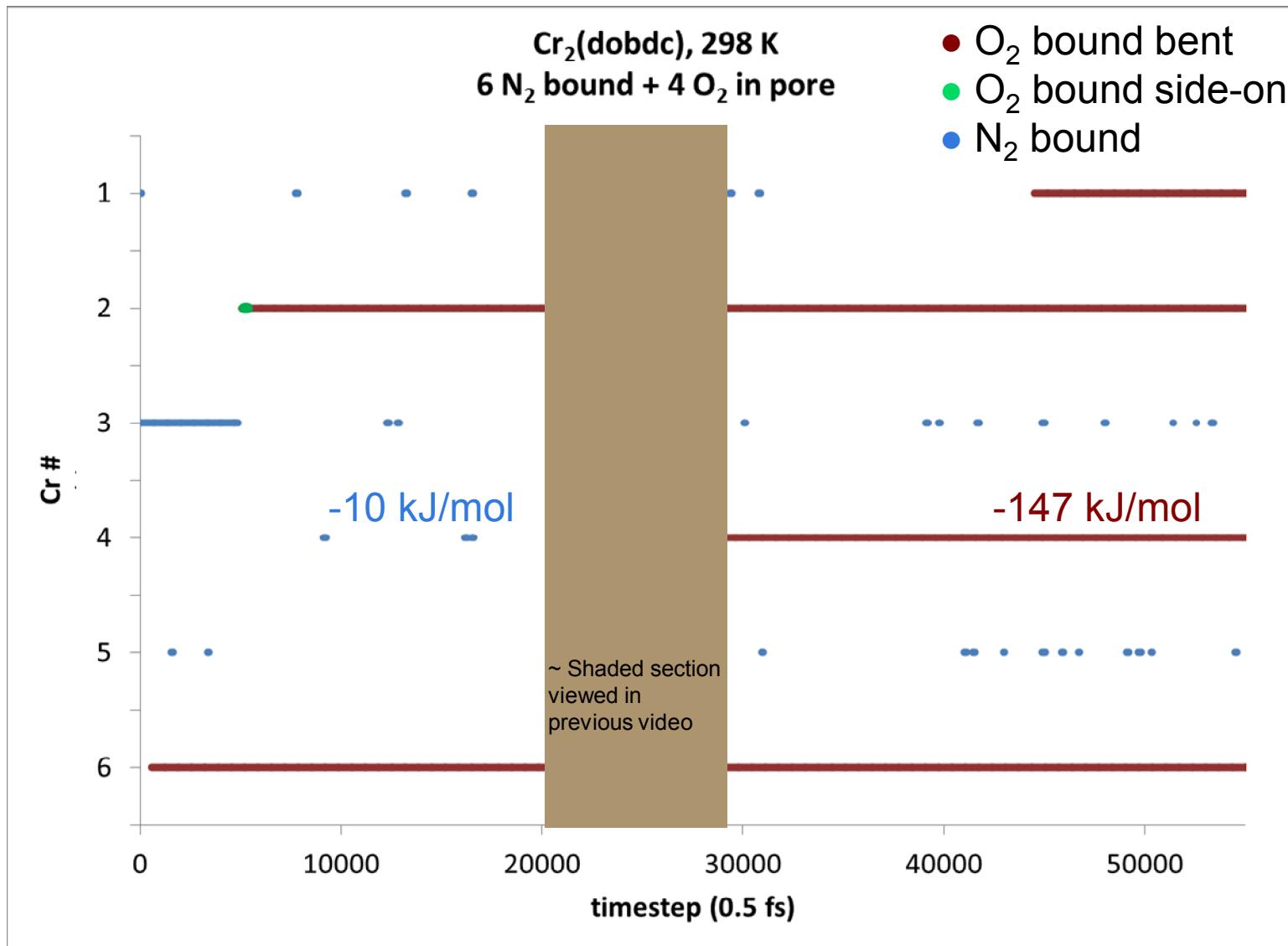
Use of Strongest *Side-On Binding* Predictions

Binding Energy Calculated as a Function of Metal Site

$$\Delta\Delta E = -(\Delta E_{O_2} - \Delta E_{N_2})$$

Side-on bonded O_2

Legend:
- M3(btc)2 ΔΔE
- M2(dobdc) ΔΔE
- M3(btc)2 O2 ΔE
- M2(dobdc) O2 ΔE
- M3(btc)2 N2 ΔE
- M2(dobdc) N2 ΔE

| 21 Sc | 22 Ti | 23 V | 24 Cr | 25 Mn | 26 Fe | 27 Co | 28 Ni | 29 Cu | 30 Zn |

tmnenof@sandia.gov
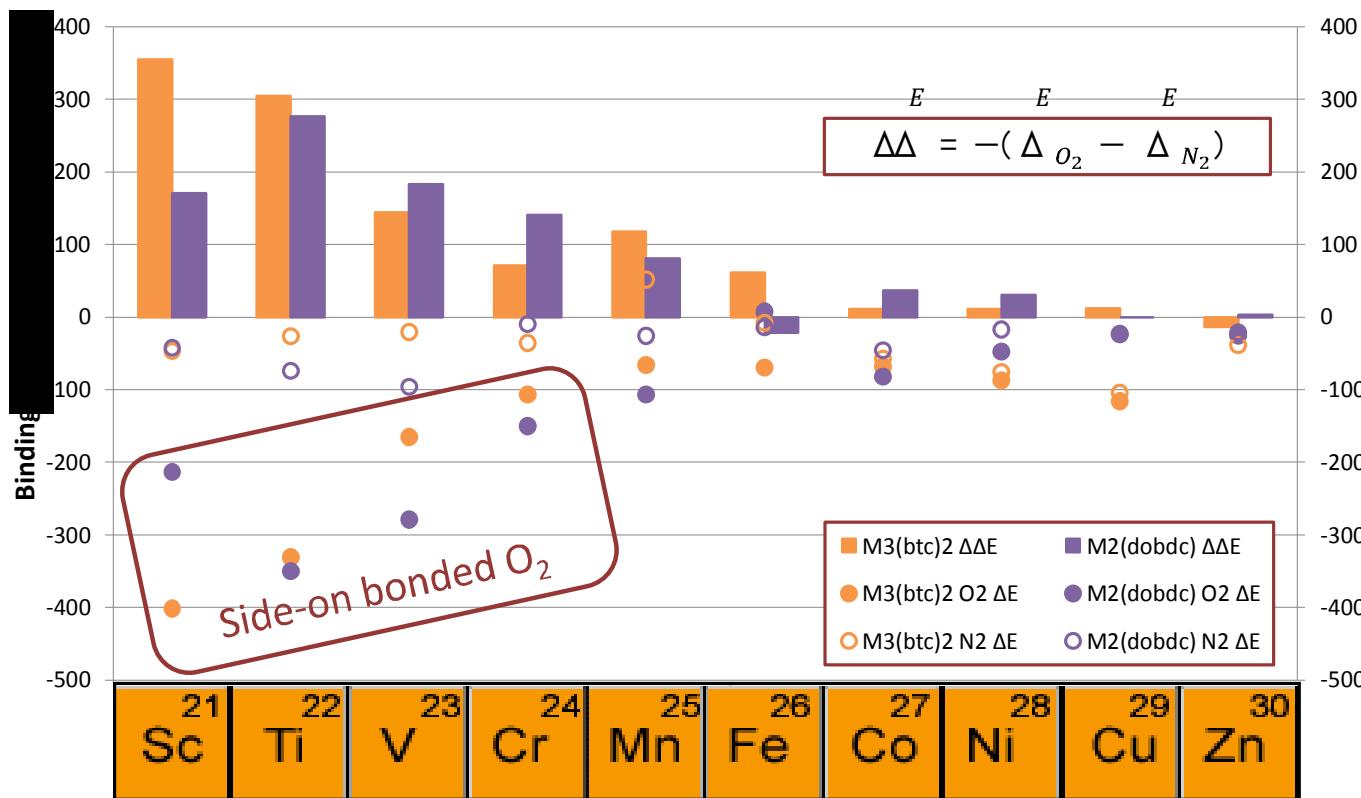
Sc-MIL-100

Unique synthesis:

Mixed $Sc(NO_3)_3 \cdot xH_2O$ and 1,3,5–benzetricarboxylic acid in N,N'-dimethylformamide and HCl.

Heated to 373K overnight

HV	mag	WD	det	Lens Mode	curr	5 μm
20.0 kV	17 647 x	5.1 mm	ETD	Field-Free	6.1 nA	Sandia National Labs

Sava Gallis, D. F., Greathouse, J.A.; Rodriguez, M.A.; Parkes, M.V.; Chapman, K.W.; Nenoff, T.M. *Chem. Mater*. **2016**, 28(10), 3327-3336 .

tmnenof@sandia.gov
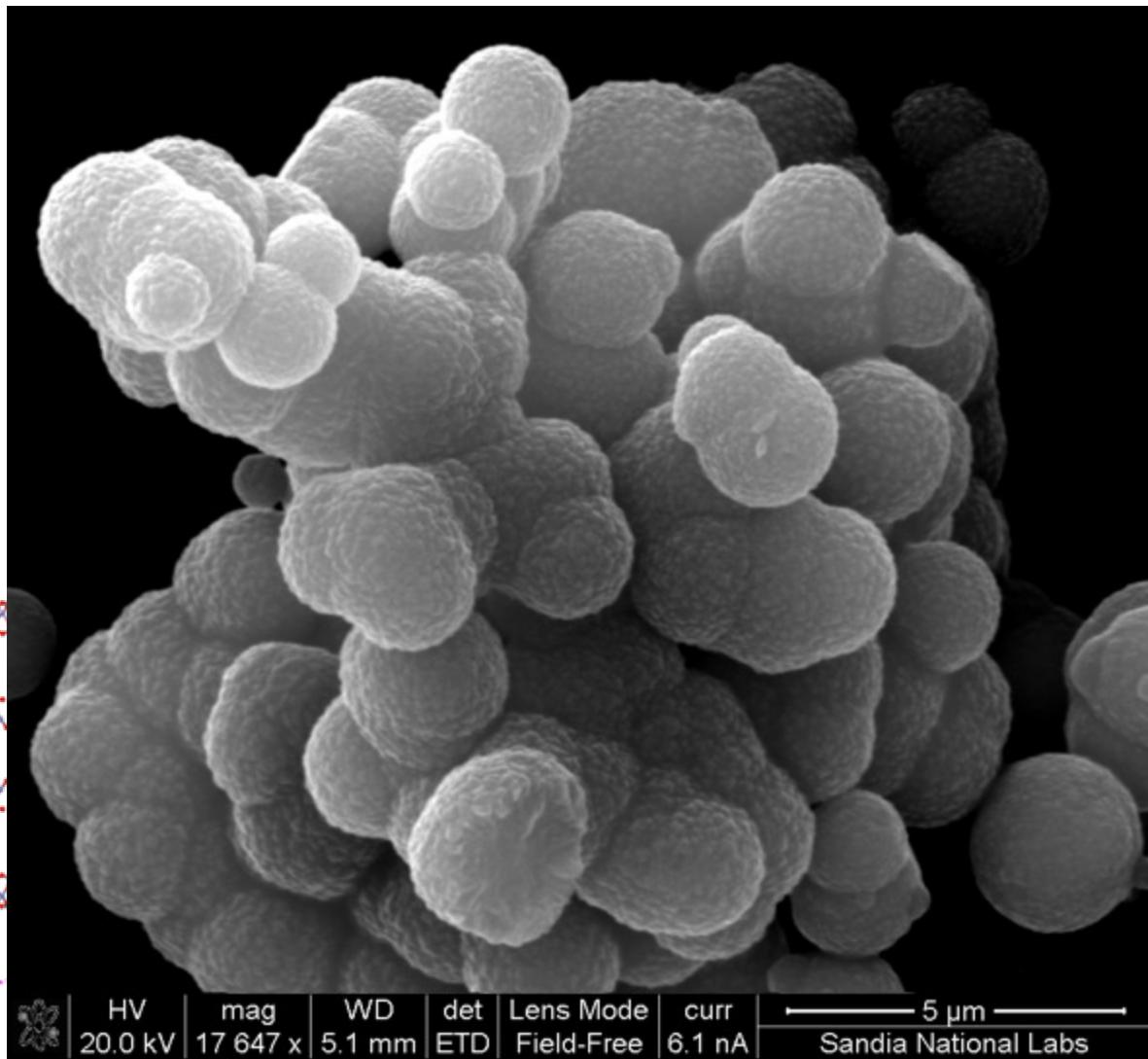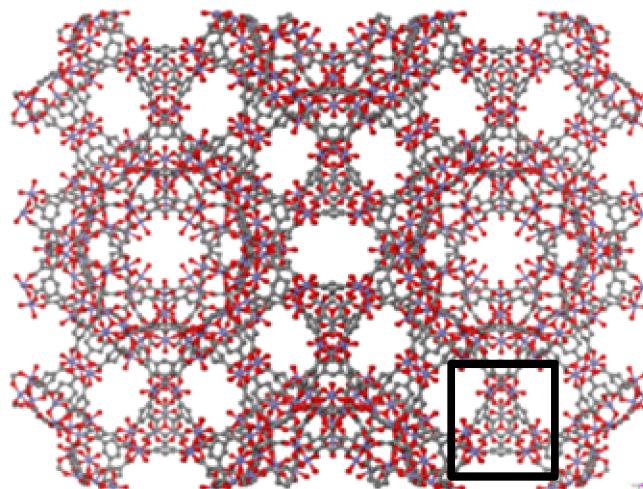
Sc-MIL-100:   Stable MOF framework over Wide Temp Range and Exposure to Variety of Gases

XRD

As synthesized
After O_2 sorption @ 313K
After N_2 sorption @ 313K

TGA-MS

H_2O

CO_2

Universal V4.5A TA Instrum

BET Surface Area Plot
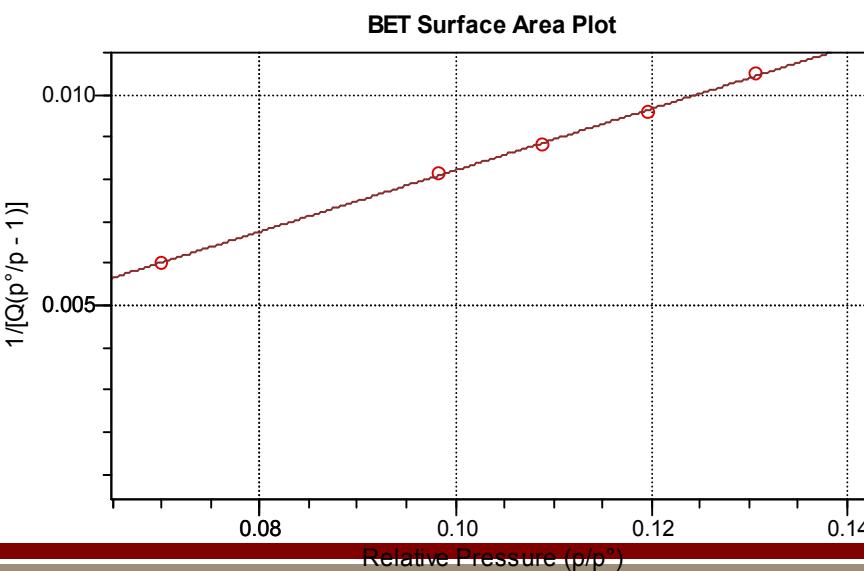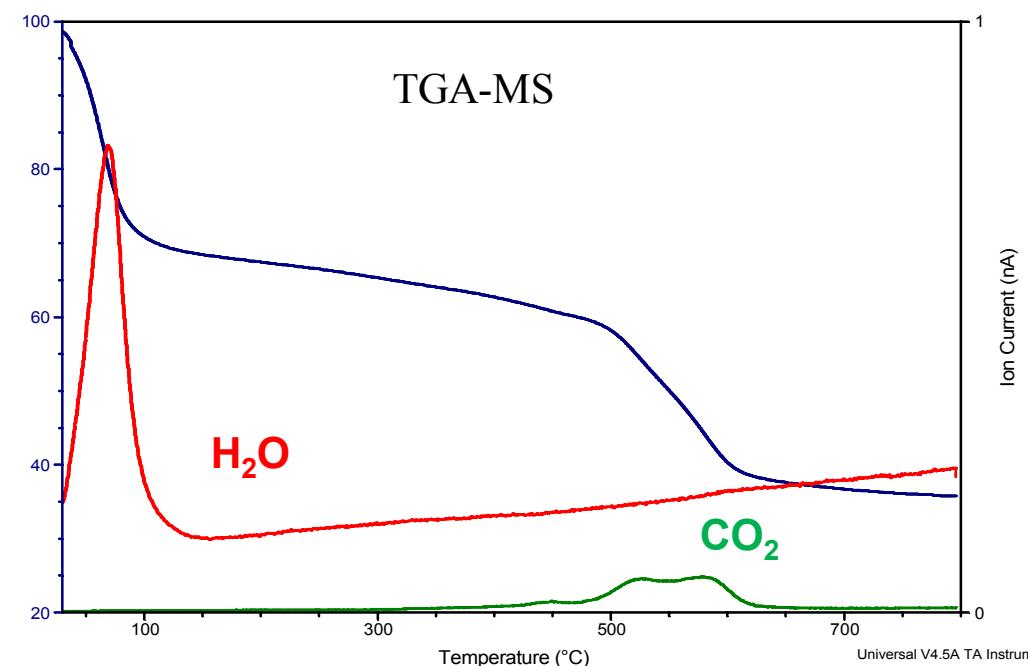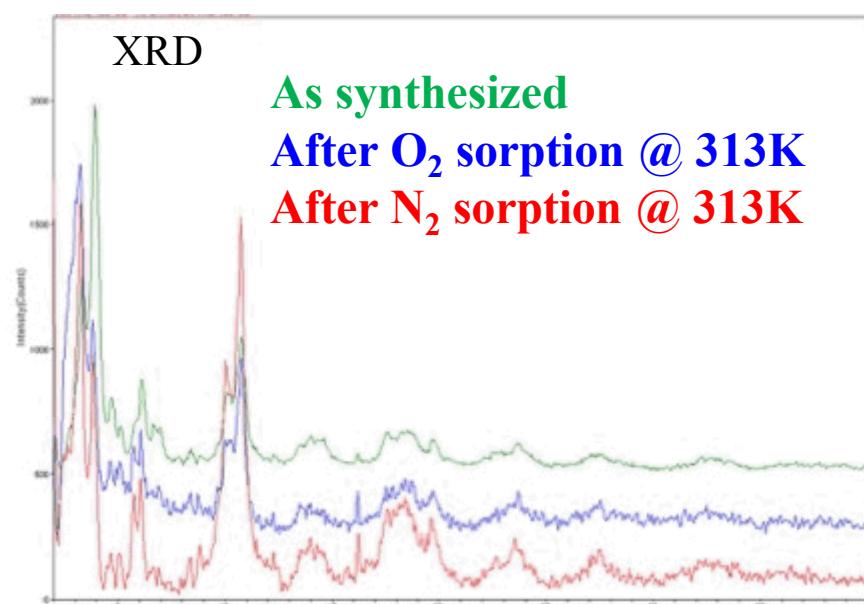
BET surface area:
1321.7194 ± 24.4623 m²/g

High Surface Area with Accessible Metal Centers

Enhanced adsorption of O_2 vs. N_2 at 77K

O_2@77K

N_2@77K
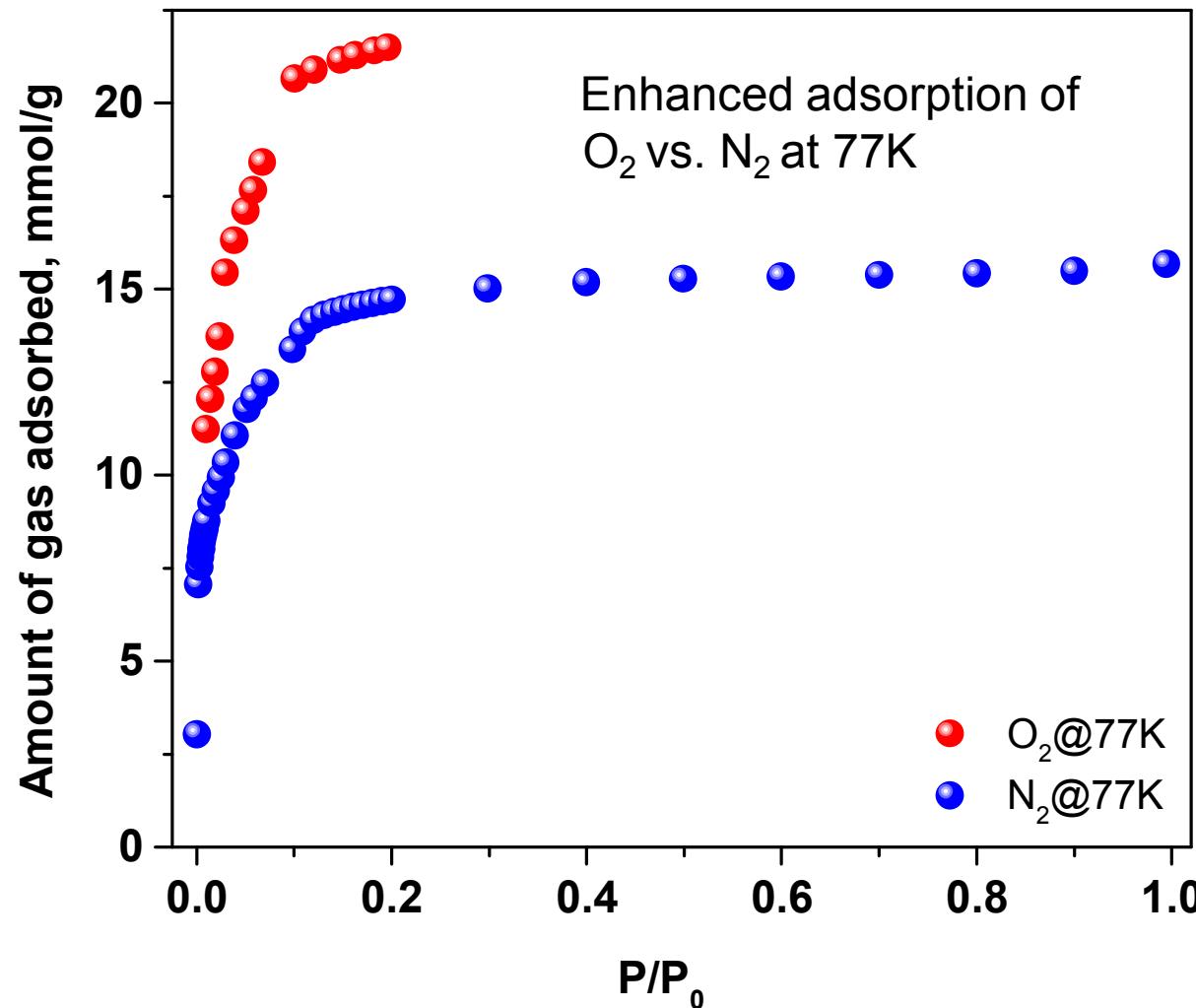
How does Sc-MIL-100 behave at more realistic operational temperatures?

- **Grand Canonical Monte Carlo (GCMC) Simulations**
- Pure gas (N_2 or O_2) adsorption over pressure range 0 - 1 bar.
- Temperature range matched with experiment: 258 K, 298 K, 313 K.
- Grand canonical ensemble (constant chemical potential, temperature, volume) using the Towhee code (Martin, *Mol. Sim.* **2013**, 39, 1212).
- Gas-gas and MOF-gas interaction energies include van der Waals and electrostatic interactions.
- Framework atoms kept at their crystallographic coordinates.
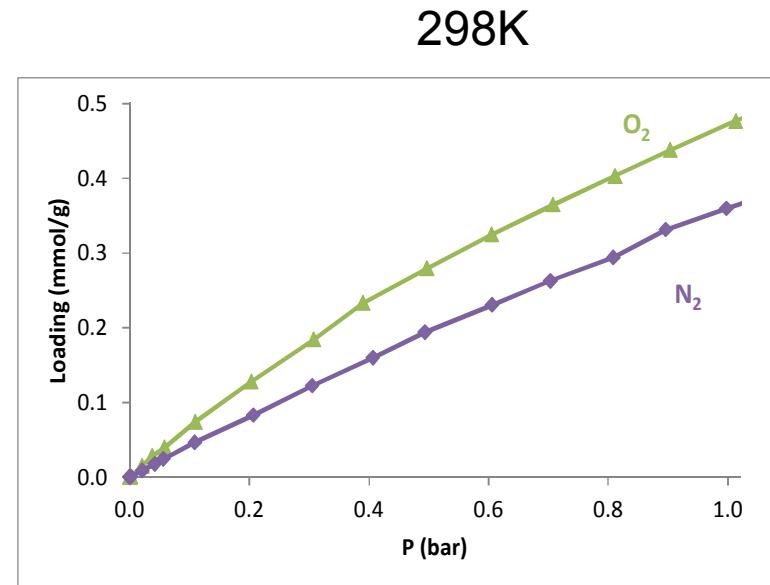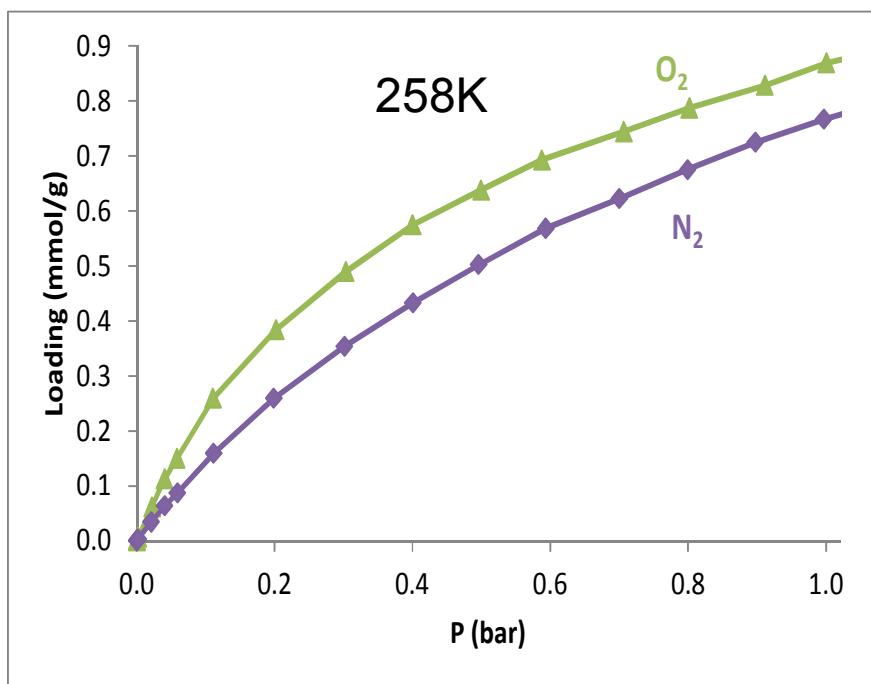
Preferred O_2 uptake but O_2/N_2 selectivity increases between 258K and 298K

21

Simulations of Competitive Gas Adsorption: based on GCMC data, 298K
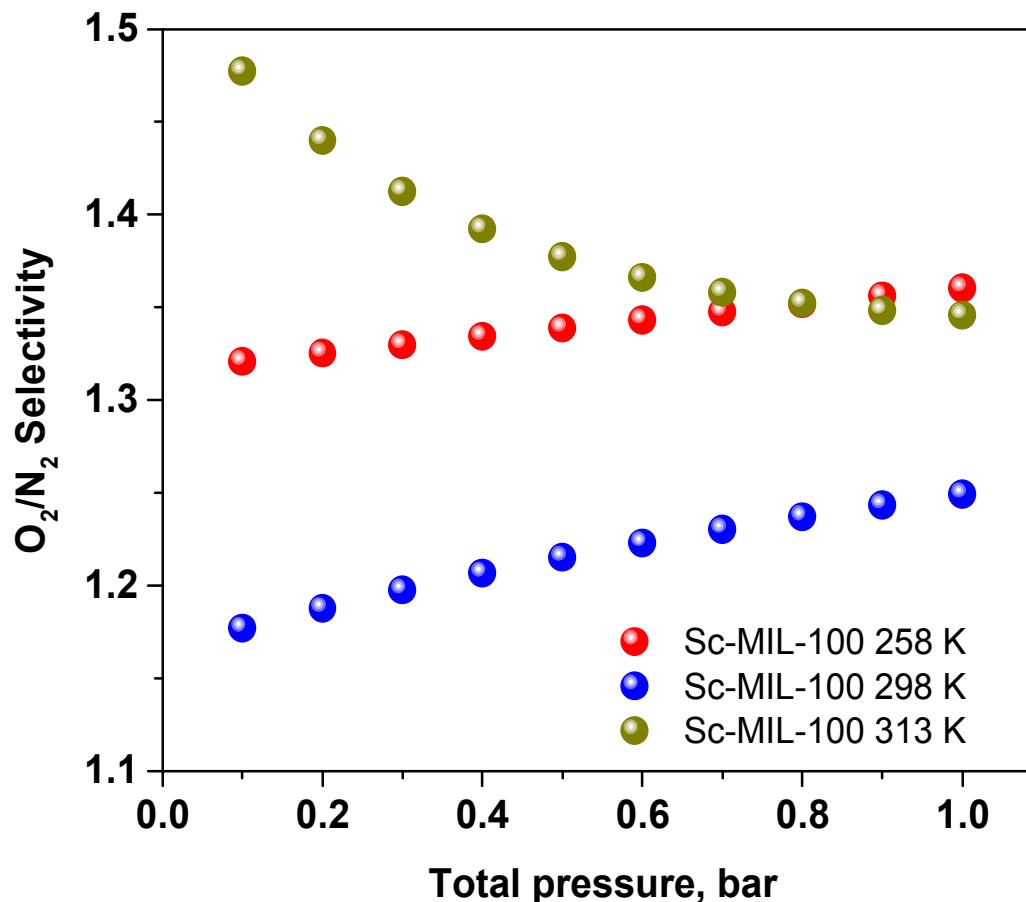
Ideal Adsorbed Solution Theory (IAST) used to calculate mixture adsorption and O_2/N_2 selectivity for **20:80 mixture (O_2:N_2)**.

Sc-MIL-100: Enhanced Quantity of O_2 vs N_2 Adsorbed over Wide Temperature Range (at least to 313K)

—— Fit using the virial eq.
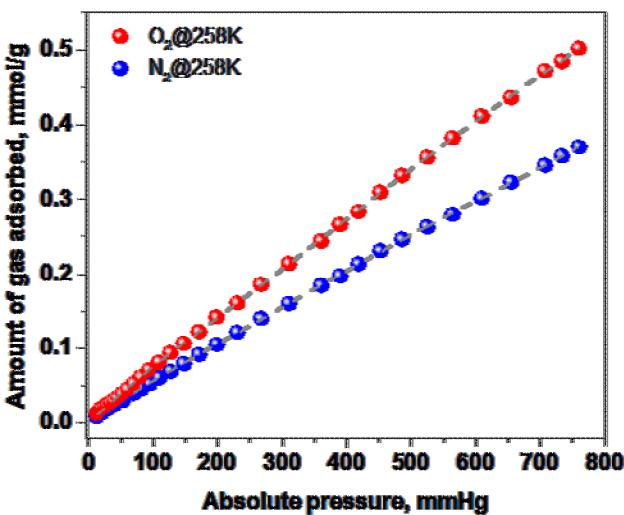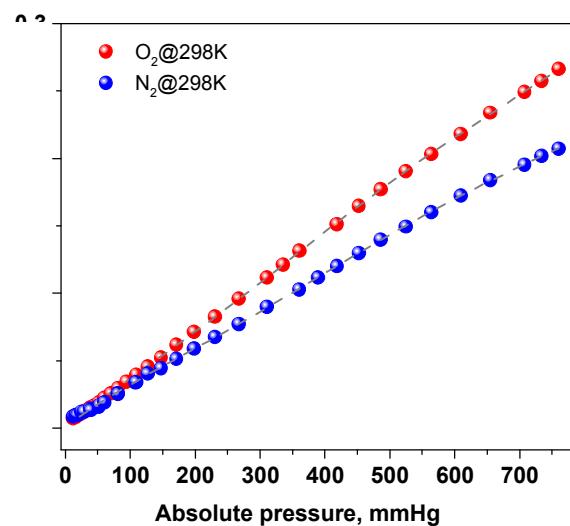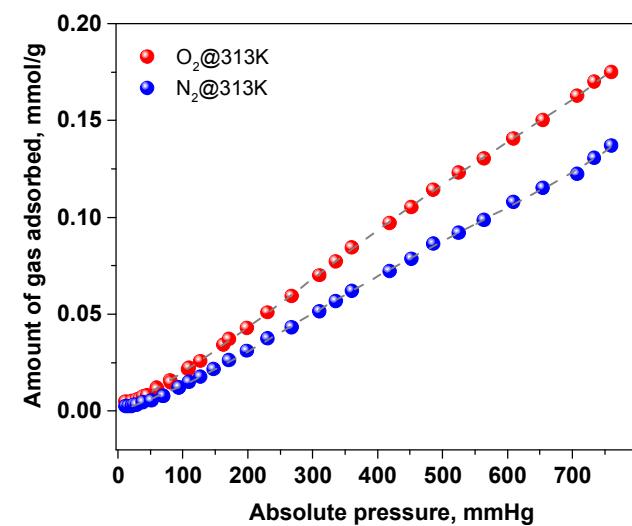
O_2 vs. N_2 @**258K** O_2 vs. N_2 @**298K** O_2 vs. N_2 @**313K**

Isotherm trends mimic those predicted by GCMC

Qst derived from 258K, 298K and 313 K
Independent Virial Fit HOA

Sc-MIL-100 Performance:
O$_2$ adsorption & Desorption over 10 cycles, 298 K, 1 atm
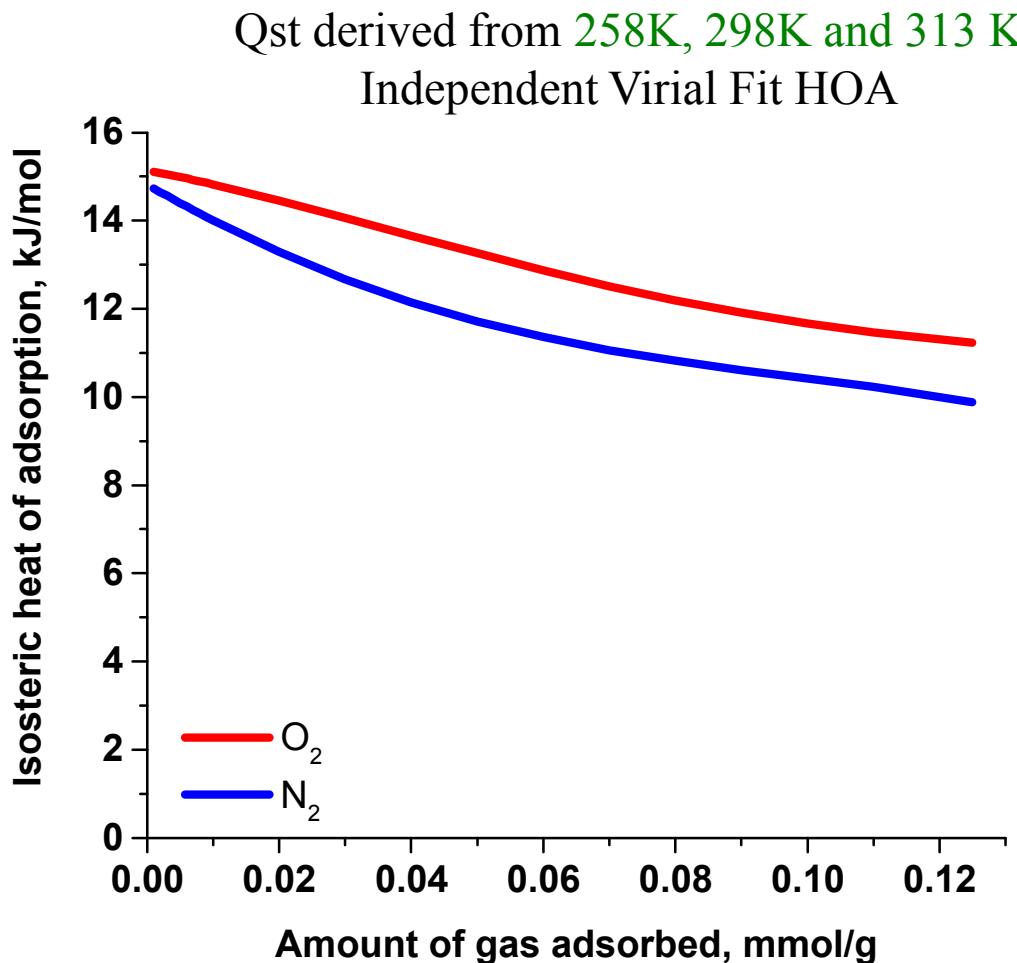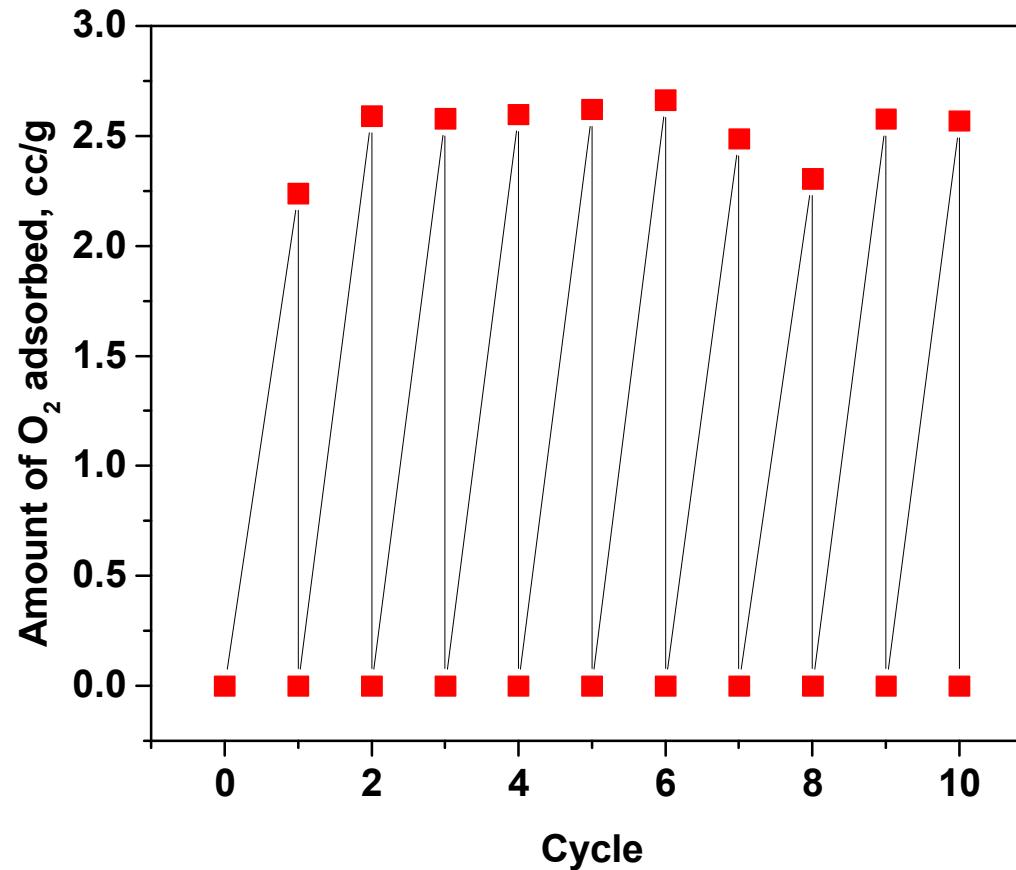
What about the structure is making Sc-MIL-100 O$_2$ strongly sorbing?

tmnenof@sandia.gov

Structure-Property Relationship Understanding of Sc-MIL-100 Oxygen Selectivity

High Energy Synchrotron X-ray, APS/ANL

Reduced Sc-MIL-100
Crystallinity is important.
Reitveld Refinement
not successful until this study.
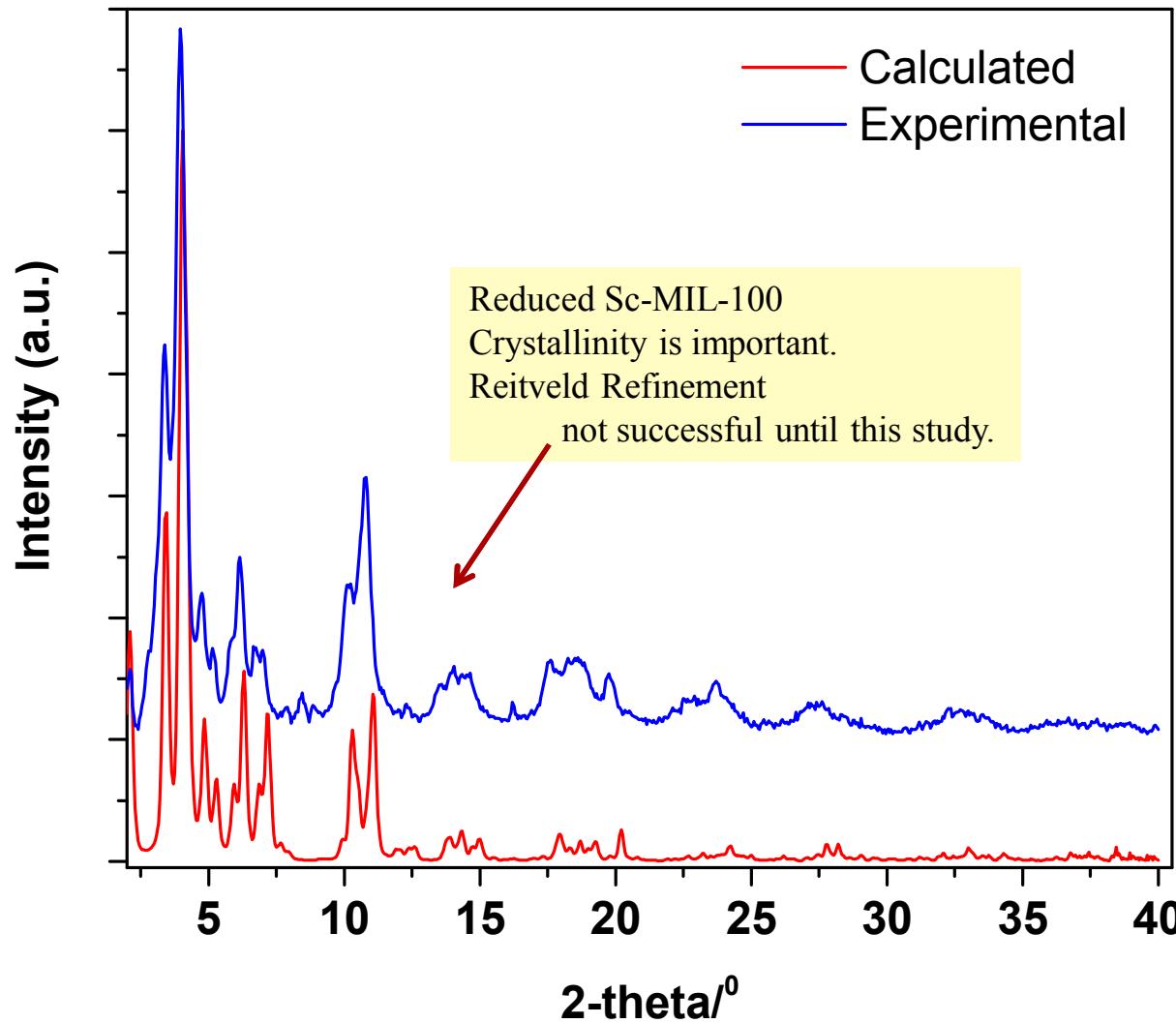
Structure-Property Analysis:
Pair Distribution Function (PDF) Analysis

> *The PDF, **G(r)**, is related to the **probability** of finding an atom at a distance **r** from a reference atom.*
> It is the Fourier transform of the total structure factor, **S(Q)**.

$$G(r) = 4\pi r\, \rho_0 [\underbrace{g(r)}_{\text{probability}} - 1] = (2/\pi)\int Q[\underbrace{S(Q)}_{\text{structure factor}} - 1]\sin(Qr)dQ$$

The structure factor, **S(Q)**, is related to coherent part of the diffraction intensity

$$S(Q) = 1 + [\underbrace{I^{coh}(Q)}_{\substack{\text{diffraction intensity} \\ \text{(corrected)}}} - \sum c_i |f_i(Q)|^2]/\, |\sum c_i f_i(Q)|^2$$

Apply corrections for background, absorption, Compton & multiple scattering

Use of high energy X-rays and large area detectors key to structure resolution
Beamline 11-ID-B

PDF: Insight Into Short Range Structural Order
eg., Amorphous SiO_2 (Glass)

- a weighted histogram of ALL atom-atom distances

Si-O 1.6Å

O…O 2.6Å

Si…Si 3.2Å

$G(r)$

$$G(r) = 4\pi r[\rho(r)-\rho_0]$$

$G(r)$ / Å^{-2}

r / Å
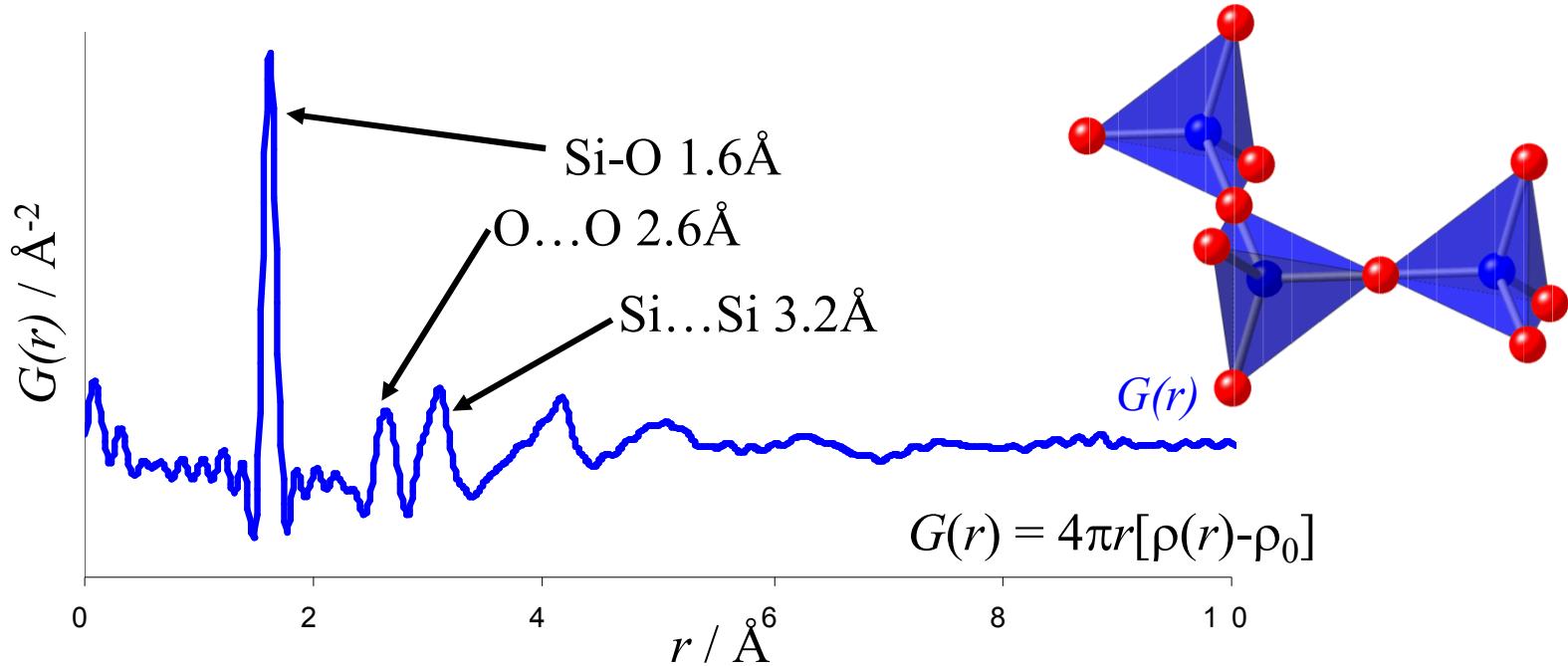
Peak position ⟺ Bond length / distance

Peak area ⟺ Coordination #, scattering intensity

Peak width ⟺ Disorder, bond angle distribution

Peak r_{max} ⟺ Particle size, coherence

Structural Modeling

tmnenof@sandia.gov

Sc-MIL-100: Structure-Property relationship evaluated using Differential (d)- PDF

d-Pair Distribution Function (d-PDF)
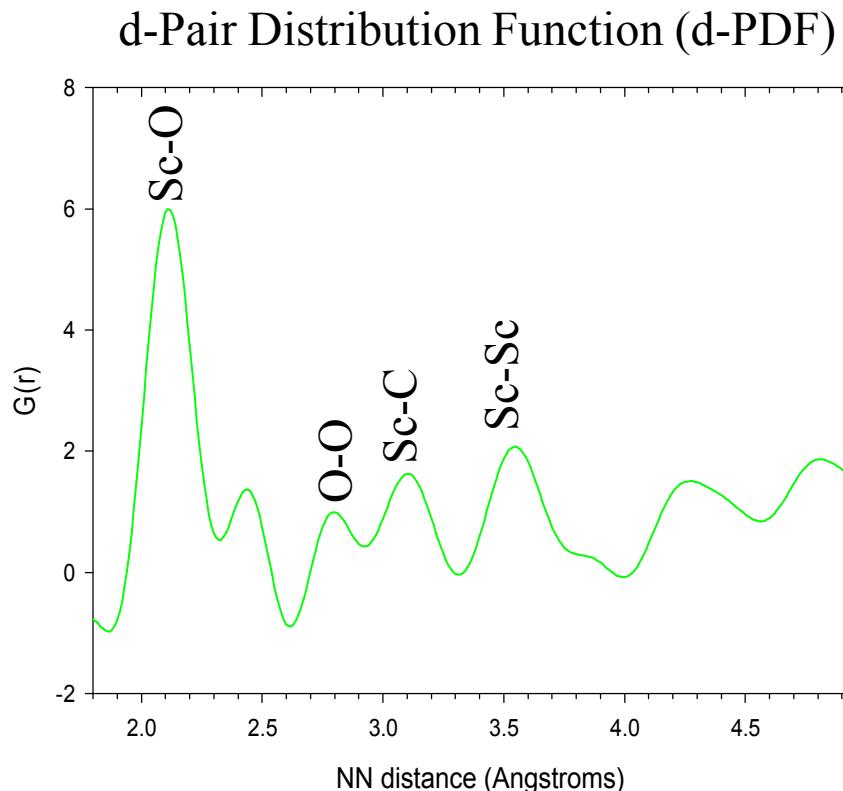
Peaks shifted to longer distances
Consistent with larger Sc incorporation
(vs. Cr-MIL-100)

d-PDF peak analysis

| Bond	NN distance (Å)	Area	FWHM (Å)
Sc-O	**2.11**	**1.5**	**0.19**
O-O	2.81	0.3	0.22
Sc-C	3.08	0.8	0.26
Sc-Sc	3.53	0.5	0.24

- Oxo-centered trimers at nodes of MIL-100 framework inferred from M-O and M…M distances

- Narrow Sc-O peak = narrow Distribution of bond lengths

- Single M-O bond length (M-O(μ_3) or M-O (carboxylate)), suggests **M-O-M angle of 113°** << 120° of a planer trimer

29

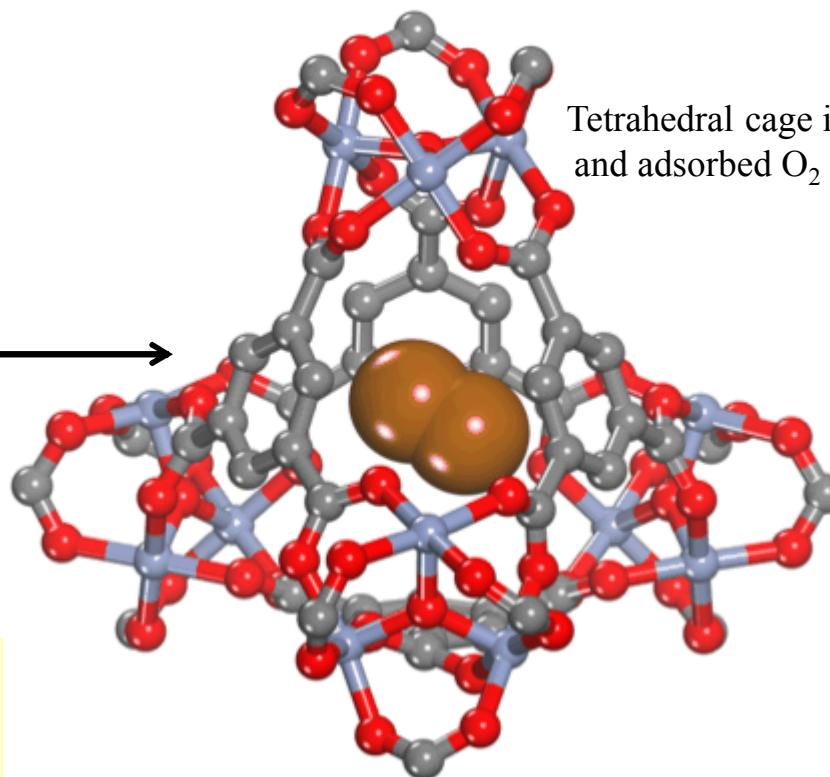Large size of Sc atom requires **out of plane distortion** in the ozo trimer of the O(μ3) atom.

Resultant "**puckering**" of trimer and "bending" of ligand is
        probable route for enhanced O_2 sorption / insertion in Sc-MIL-100

"tulip opening"

Sc   Fe
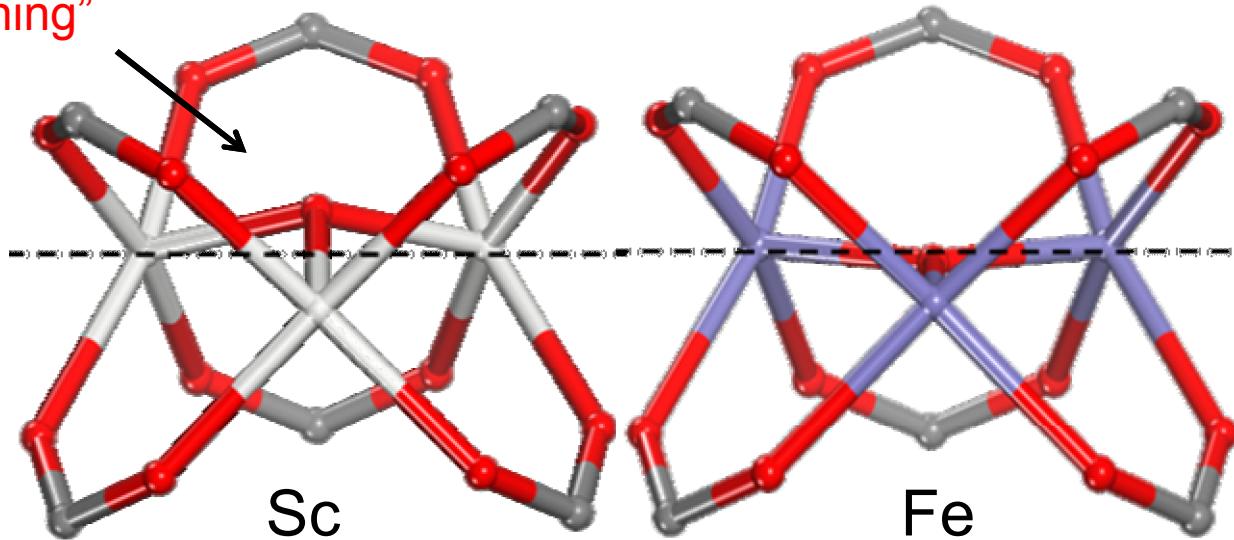
Rietveld refinement unit cell for Sc-MIL-100: a = 74.518(31) Å, R = 10.7%
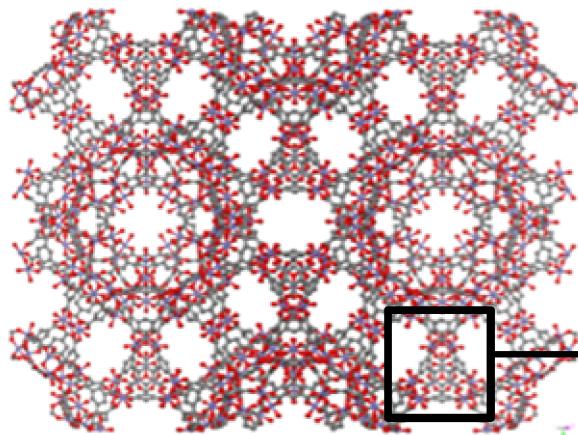
Tetrahedral cage in the MIL-100 framework and adsorbed O_2 molecule (large spheres).

GCMC-equilibrated configurations:
Cage and pore occupancy
as determined at 298K and 1 bar

P (bar)	Gas	# in Cage	# in Pore	Total
1	N_2	21	27	48
1	O_2	47	20	67

31

Conclusions

- Multidisciplinary teaming allows for in-depth understanding of materials structure-properties

- The collaborative use of DFT and AIMD enabled the prediction and understanding of metals needed in MOFs for selective gas binding

- **Sc-MIL-100**: Early transition metal MOFs show preference for O_2 vs N_2 over wide temperature range (up to at least 313K), as confirmed by isosteric heats of adsorption.

- Modeling pointed us toward Sc based MOFs for O_2 preferential adsorption, chemistry, crystallography, & gas testing explained why the material worked well.

- On-going Research:
  Techno-economic Analysis Model for ion exchange resins in silica removal from Industrial Water Recycle and
  Burner Design to Oxyfuel combustion applications
  Novel MOFs designed for Fission Gas Separations

Sandia National Labs:

Campus Recruiting

Sandia is a National Laboratory

Sandia National Laboratories

Sandia National Laboratories

Science labs

Nuclear energy lab

Fossil energy lab

Energy efficiency and renewable energy lab
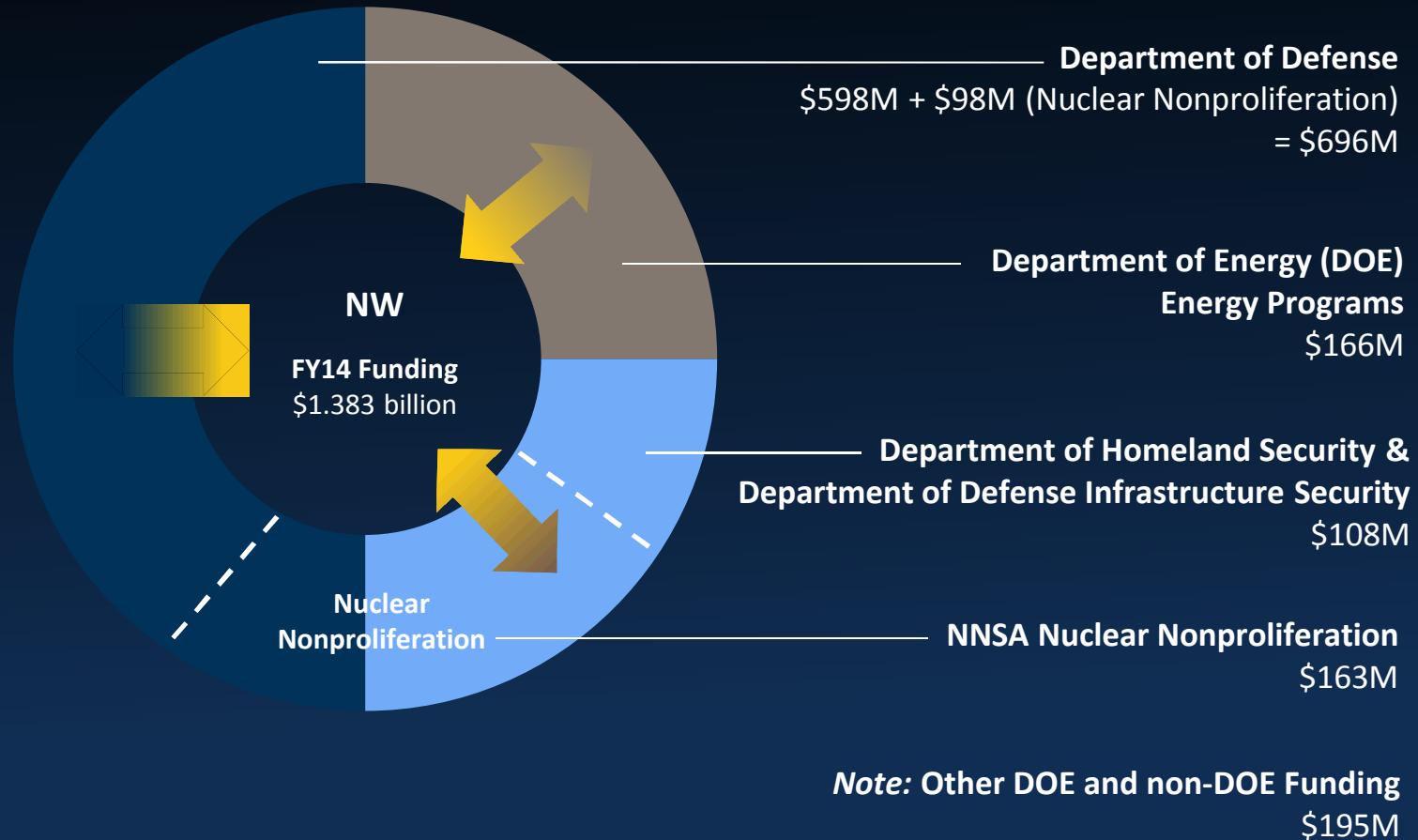
Sandia has two main locations

Sandia National Laboratories

Sandia National Laboratories

Legend:
- Administration labs
- Science labs
- Nuclear energy lab
- Fossil energy lab
- Energy efficiency and renewable energy lab

Sandia's Funding - ~ $2.5 Billion

NW

FY14 Funding
$1.383 billion

Nuclear
Nonproliferation

Department of Defense
$598M + $98M (Nuclear Nonproliferation)
= $696M

Department of Energy (DOE)
Energy Programs
$166M

Department of Homeland Security &
Department of Defense Infrastructure Security
$108M

NNSA Nuclear Nonproliferation
$163M

Note: **Other DOE and non-DOE Funding**
$195M

High reliability, high consequence of failure, challenging environments, and technology solutions

Our Workforce   ~11,700 employees

~**10,300** Regular employees

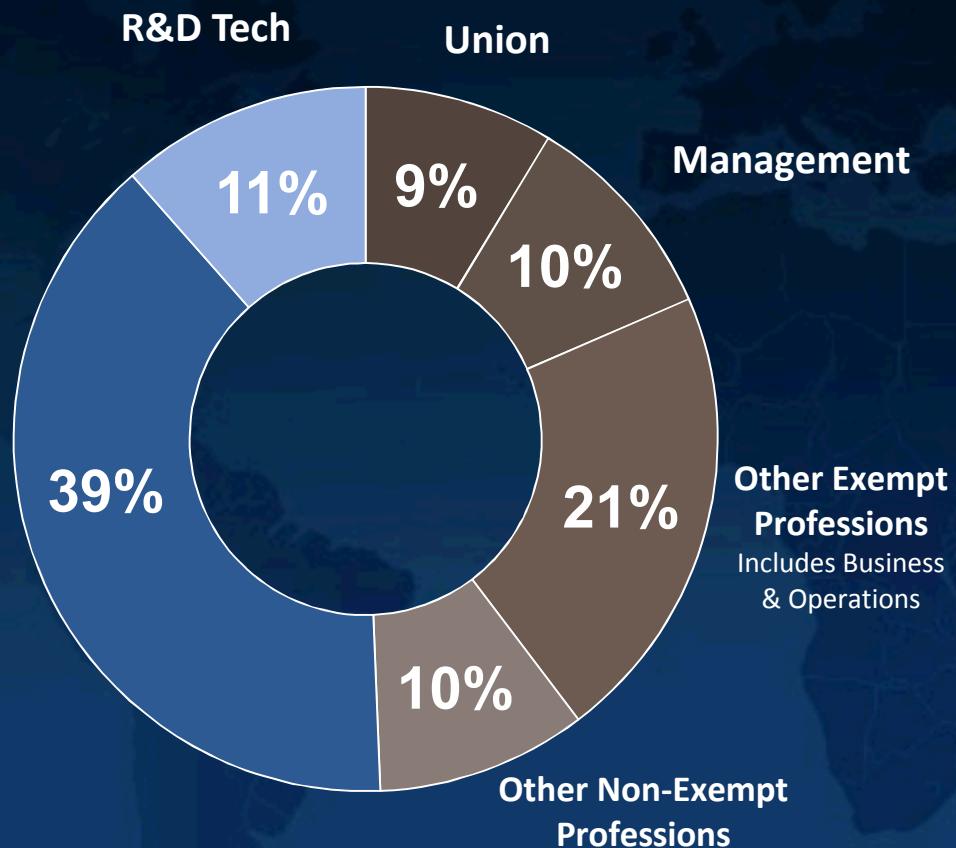~**1,400** Temporary employees, students & postdoctoral appointees

New Mexico Site:

Workforce: ~10,500

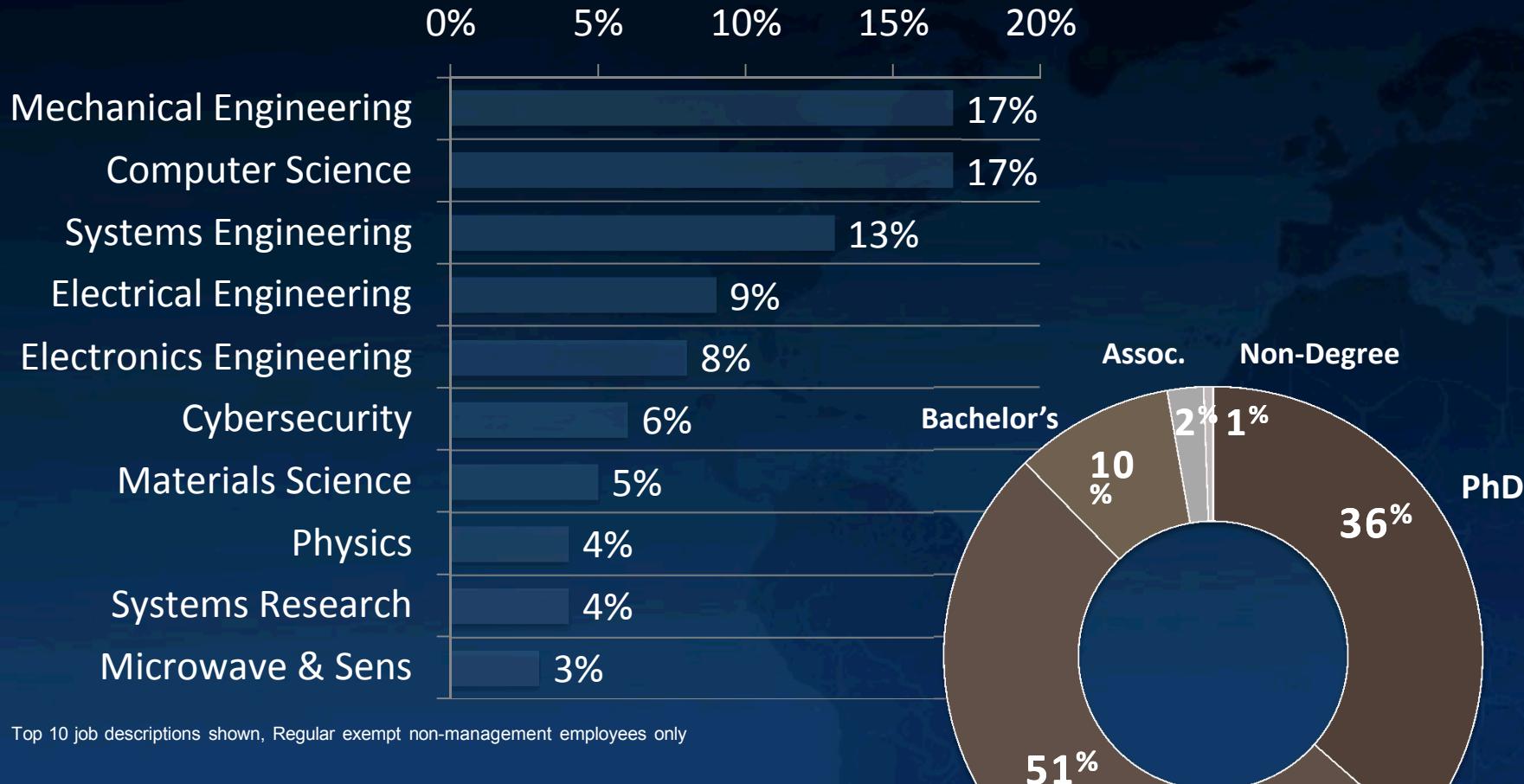R&D employees: ~4,700

(R&D Staff & Technologists)

California Site:

Workforce : ~1,200

R&D employees: ~600
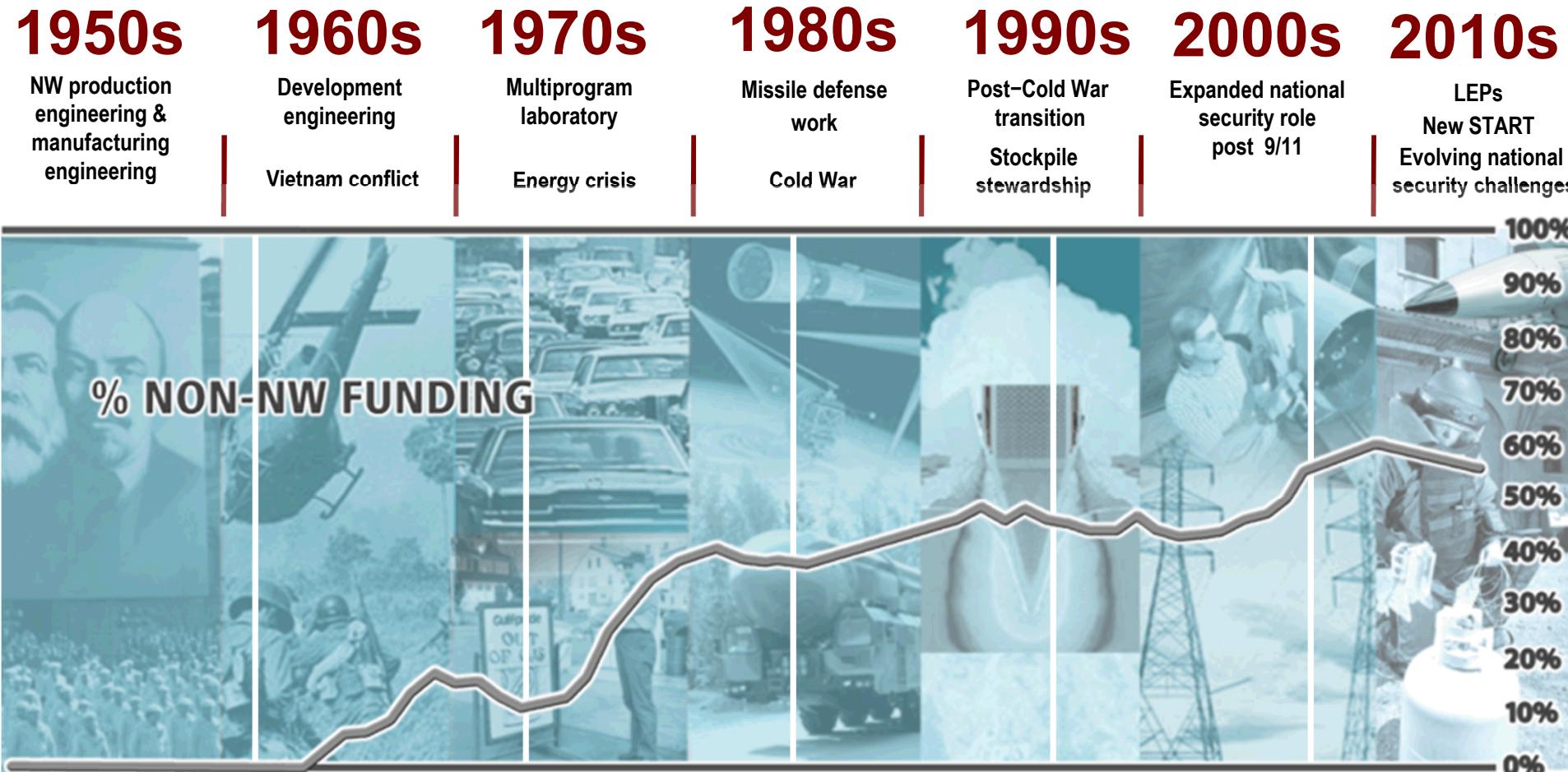
(R&D Staff & Technologists)

R&D Tech

Union

Management

Other Exempt Professions
Includes Business & Operations

Other Non-Exempt Professions

&D Staff

11%

9%

10%

39%

21%

10%

R&D by Discipline & Degree

Discipline	Percentage
Mechanical Engineering	17%
Computer Science	17%
Systems Engineering	13%
Electrical Engineering	9%
Electronics Engineering	8%
Cybersecurity	6%
Materials Science	5%
Physics	4%
Systems Research	4%
Microwave & Sens	3%

Top 10 job descriptions shown, Regular exempt non-management employees only

Degree breakdown:
- PhD: 36%
- Master's: 51%
- Bachelor's: 10%
- Assoc.: 2%
- Non-Degree: 1%

Sandia's Mission Work Reflects the Nation's Security Challenges

1950s	1960s	1970s	1980s	1990s	2000s	2010s
NW production engineering & manufacturing engineering	Development engineering	Multiprogram laboratory	Missile defense work	Post–Cold War transition	Expanded national security role post 9/11	LEPs New START Evolving national security challenges
	Vietnam conflict	Energy crisis	Cold War	Stockpile stewardship		

% NON-NW FUNDING

100%
90%
80%
70%
60%
50%
40%
30%
20%
10%
0%

Examples of Sandia's Impact

Portable Diagnostic Device for Bacillus Anthracis Detection in Ultra-Low Resource Environments

Ebola Outbreak
Sandia contributes to global response of Ebola outbreak by developing a sample delivery system cutting the wait time and potentially fatal exposure.

Anthrax Detection
Sandia developed a pocket-sized cartridge to sense concentrations of virulent B. anthracis, the bacteria that causes anthrax infection.

Fukushima Quake*
Sandia developed Cs$^+$ specific exchange resins to clean up radioactive wastewater.

Detecting IEDs
Combat personnel now have a new tool for uncovering improvised explosive devices: Sandia's highly modified miniature synthetic aperture radar system, which is being transferred to the U.S. Army.

Hurricane Katrina
Sandia is called to assess flooding and infrastructure failures.

9/11
Sandia sets contingency plans for release of materials and aircraft attacks on critical facilities immediately after 9/11. Search dogs are equipped with cameras for search and rescue K-9 handlers.

Mission Foundations R&D

Mission driven innovation enabling mission area success
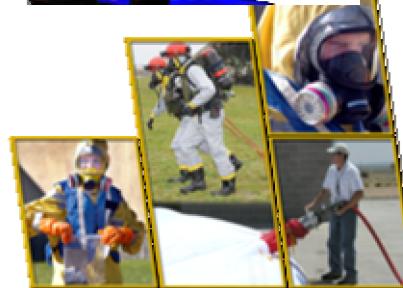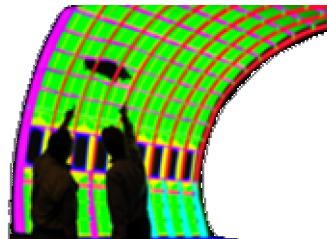
Nuclear Weapons	Energy and Climate	International, Homeland, and Nuclear Security	Defense Systems and Assessments

LDRD Research Foundation Disciplines

Research Disciplines that Enable Capabilities

Strong research foundations play a differentiating role in our mission delivery
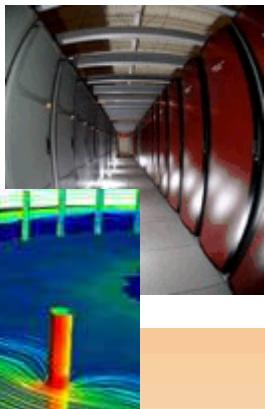
High Performance Computing
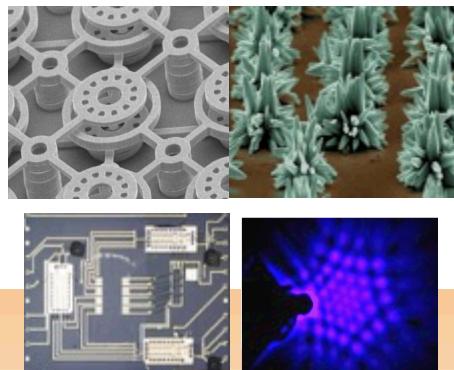
Nanotechnologies & Microsystems

Extreme Environments

Large Scale Testing

Computing & Information Sciences	Radiation Effects & High Energy Density Science	Materials Science	Engineering Sciences	Geoscience	Nanodevices & Microsystems	Bioscience	New Ideas
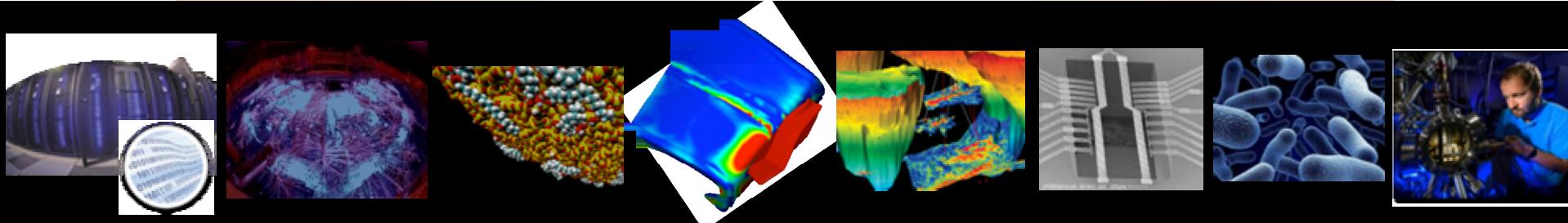
LDRD Research Foundation Disciplines

Example 1: Novel Functionalized Materials, Synthesis & Application

Materials assurance & engineered materials with tailored functionality for operational environment.

New materials designed for operational environment with easier manufacturing and reduced costs.

Using computational materials and chemistry capabilities, we synthesize functionally new materials with novel properties and controlled microstructure tailored to the operational need.

Generic Spray Device

Coating

Substrate
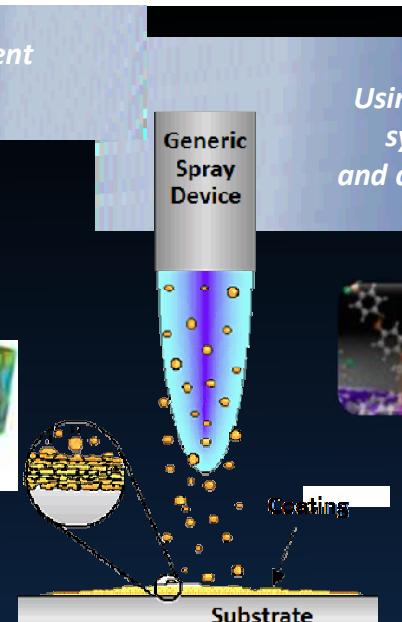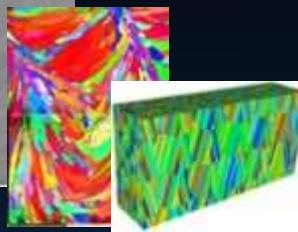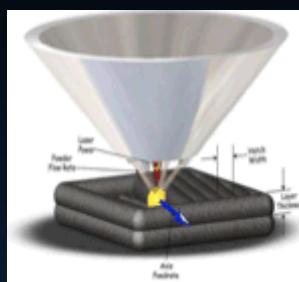
Versatile thermal spray manufacturing for system production.
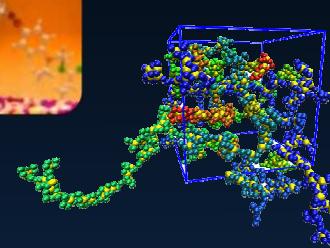
Scalable solution synthesis to create nanofibers, nanoparticle inks and suspensions to high density ceramics with controlled microstructures and properties.

Provide robust coating technologies

113° 114° 127° 145°
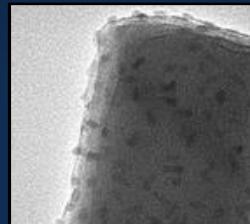
Biomimetic assembly and tailoring of molecular architecture to functionalize surfaces and structures.

ZnO via Multi-stage Growth

Designer peptide synthesis used to tailor molecular function.

Example 2: Atoms to Continuum Characterization

Material forensics at all scales for design and performance assessment of new & used materials.
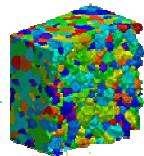
- State-of-the-art microstructural material characterization capability.
- Failure Analysis/Forensics Materials Identification/Qualification.
- Comprehensive analysis methods turning data into knowledge.
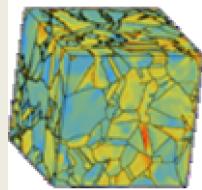
Performance can be improved when we understand composition, condition, and structure of all material types, at all material scales, and through built up systems.

Multi-beam SEM

Aberration corrected TEM (STEM)
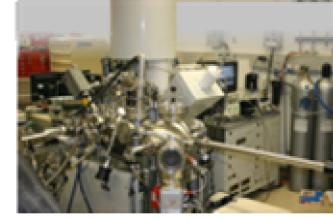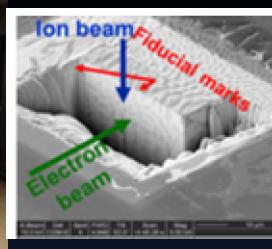
Example 3: Mission Inspired Modeling

Materials assurance, data analysis, predictability, optimization, and manufacturability.

- Materials modeling across all physical and time scales (including agin
- Science of materials failure for improved reliability.
- Predictive performance modeling across environmental spectrums.

Performance uncertainty is greatest when designed systems are exposed to harsh extreme use conditions. Predictive modelling at the right scales reduces these uncertainties!

Process → Microstructure → Performance → Design
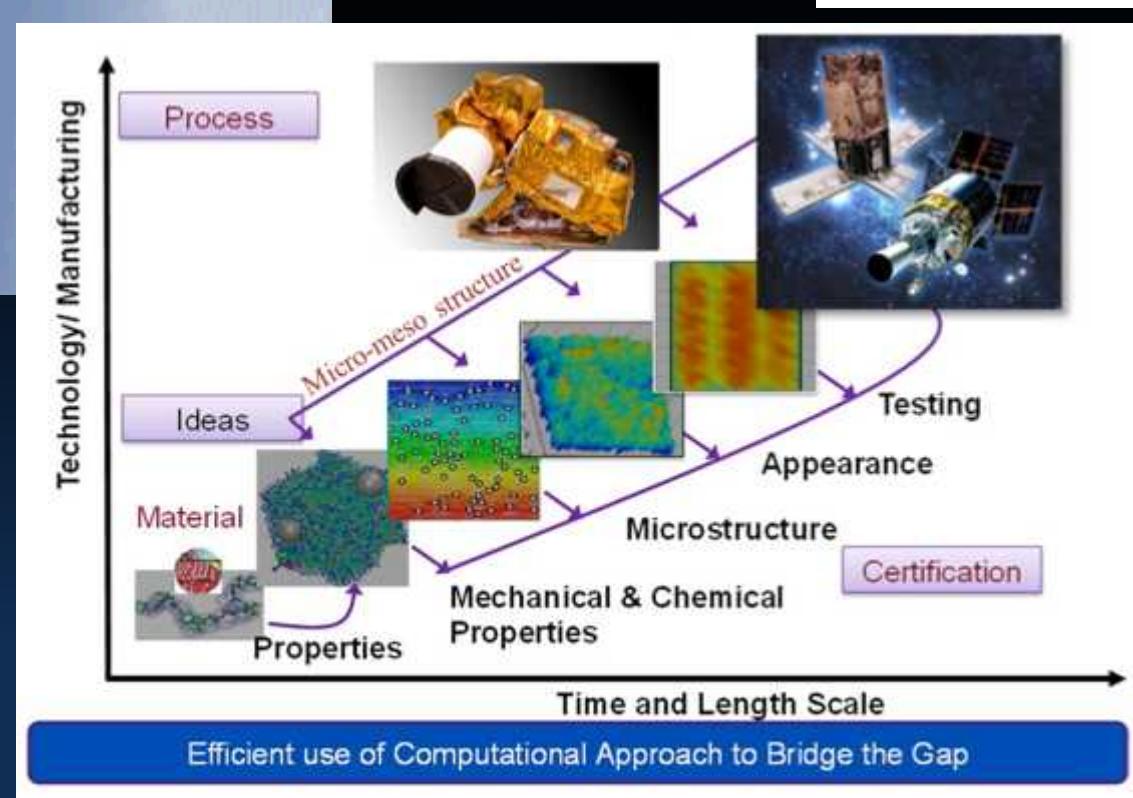
Example 4: Cradle to Grave Reliability

Science-based abilities to detect, assess, and predict materials performance and aging.

Reliability – the ability of a system or component to perform and maintain its functions in routine circumstances, *as well as* perform as expected in demanding or unexpected circumstances. **It is statistical not deterministic.**

Low Volume & High Consequence Applications
Demand Predictive Materials Reliability

- **Material variability affects …**
  - **Initial properties, and**
  - **Evolution of properties during service**
- **Collecting experimental data over lifetimes of interest creates a challenge**
- **Require experiments and modeling that reflect materials variability**
  - **Current materials models are deterministic**

Apply Online *sandia.gov/careers and*
...contact Sandians to be your champion

In addition to *Permanent Staff Positions*: Fellowship Opportunities

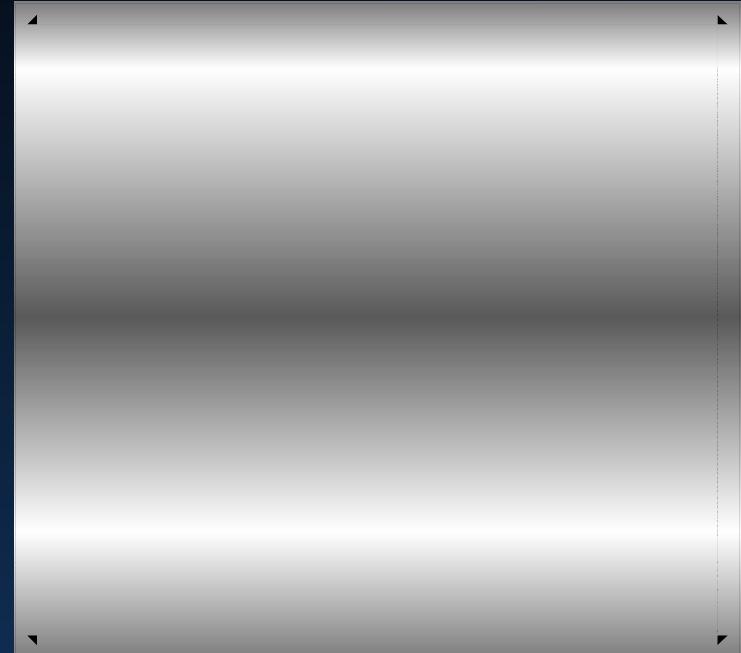**Ph.D. Level Fellowships**

- Harry S. Truman Fellowship

3 year, $110K/yr + ~$80K support funds

Oct 1 deadline

- John Von Neumann

Computational Science

1 year (+1 additional), Dec 1 deadline

Post-doc Opportunities

Key areas for post-docs at Sandia:

- Biosciences and biotechnology
- Chemistry and materials science
- Combustion
- Computational mechanics
- Computer science
- Hydrogen
- Microelectronics and microfluidics
- Nanotechnology
- Physics

Eligibility Criteria

- A recent PhD (awarded within the past five years) or the ability to complete all PhD requirements before beginning
- No previous post-doc appointments at a national laboratory

Includes:
A comprehensive benefits package including health insurance, vacation, paid holidays, and relocation assistance.

Internships

Encourages qualified students to develop interests in critical skills areas related to our mission, with the ultimate objective of developing our pipeline for our future. Available for Summer, Year Round and Co-op.

Eligibility Criteria

- Min. cumulative GPA (3.2 Undergrad/3.5 Grad)

- Have U.S. citizenship for positions that require clearance or as stated in the job posting

- Full-time enrollment status at an accredited college, university, or local high school

- At least 16 years of age
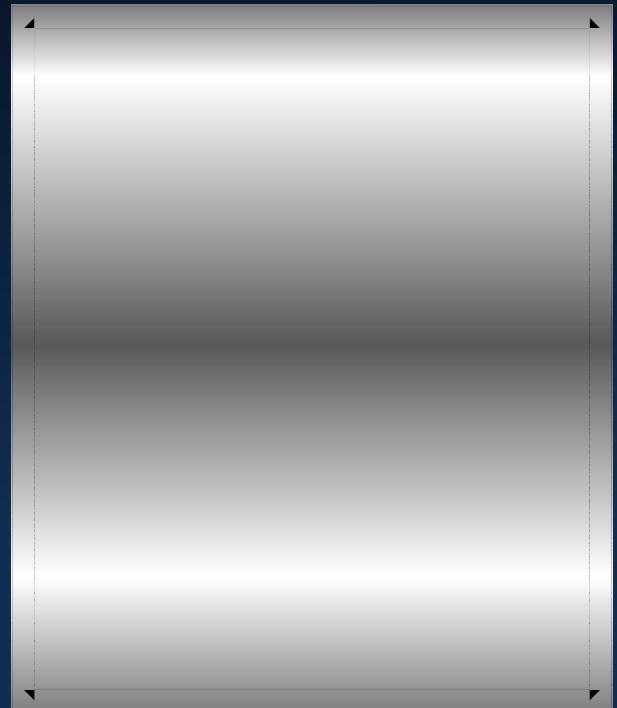
Sandia National Laboratories' Sites

Albuquerque, New Mexico

Kauai Test Facility, Hawaii

Tonopah Test Range, Nevada

Yucca Mountain Nevada

WIPP, New Mexico

Pantex, Texas

Livermore, California

51

Extra slides

Coupling of Burner design and Oxy-fuel Combustion to Radiant Heat Transfer
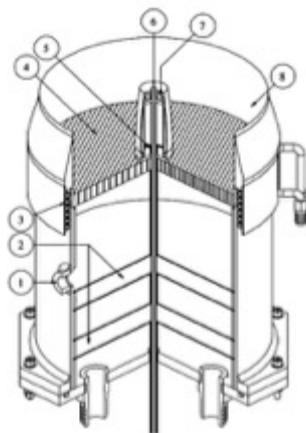
-Newly designed and constructed burner with smaller diameter inside tube for CH_4 into oxider jet flow

- Allows either premixed or non-premixed methane-air flame

- Designed specifically for pure O_2 and enriched O_2 stream as determined by gas separations data from MOFs and economic life cycle analyses
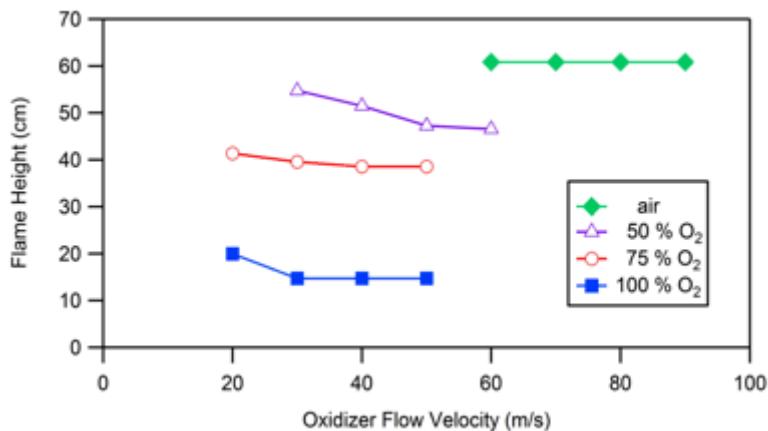
LDRD calculated/predicted flame heights when using a 1/8", 0.020 wall stainless steel tube to deliver methane to the Dunn burner.

The volumetric flow of methane is always equal to ½ the flow of oxygen, to maintain stoichiometric combustion conditions.

Preliminary Investigation of Oxygen-Enriched NG Flames

Performed preliminary testing performed with oxidizers of pure oxygen and with 50% O_2 in N_2, using an overall equivalence ratio of 1, with a constant methane flow

- Velocity (Re) of oxidizer flow is 50% lower when using pure O_2, making for taller flame (slower mixing)

- Soot formation is enhanced when using pure O_2 (higher temperatures, slower mixing)
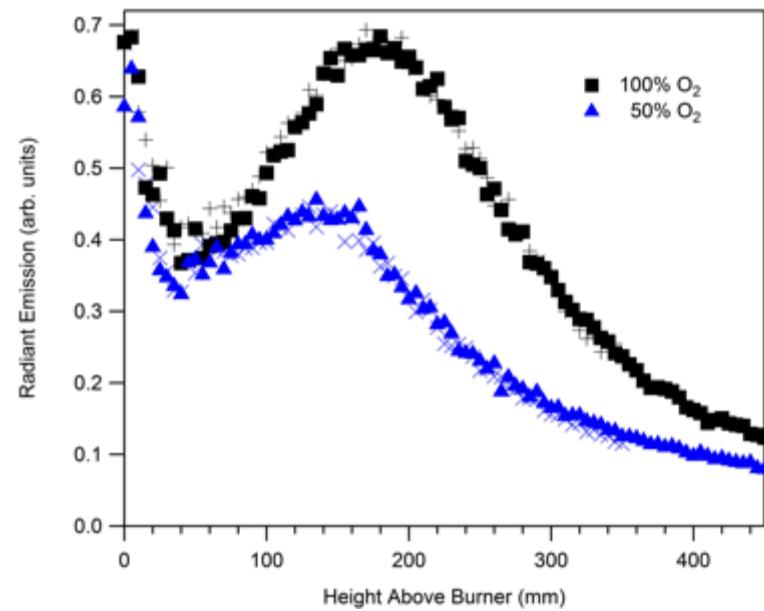
Radiant emission measurements have been performed along the flame centerline

- Data for 100% O_2 shows significantly more thermal radiation

- Flame temperatures are higher when using pure O_2 (more radiation from flame products)

- Some soot is formed in the 100% O_2 flame

50% O_2 in N_2

100% O_2

Systems Analysis of MOF-based Air Separation

MOF adsorption isotherms (N₂ & O₂) (from MOF team)
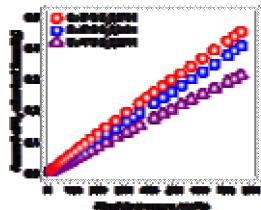
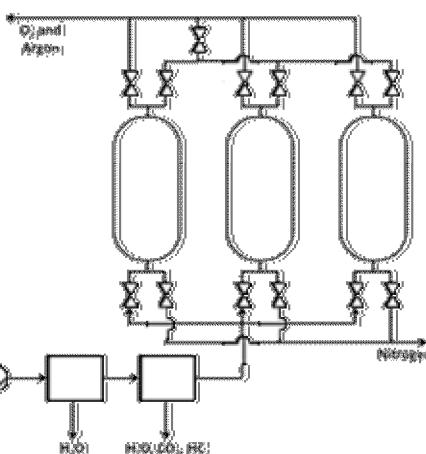Optimal O_2:N_2 ratio for combustion (from combustion team)
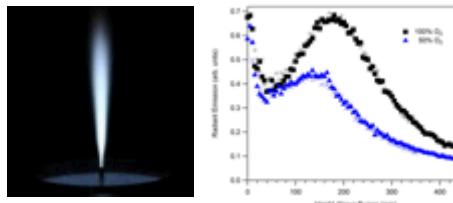
Can MOF-based PSA reduce energy consumption by 5% vs. conventional PSA air separation?

| Construct and validate model of PSA process | → | Adjust PSA model parameters to yield desired O_2:N_2 ratio | → | Estimate energy consumption based on PSA parameters |

PSA mo
Beeyani
Technol

Key PSA model parameters:

- Vessel dimensions
- Operating pressures
- Cycle time
- Feed rate

PSA energy consumption is dominated by compressor(s)
→ Operating pressures and flow rates are primary drivers

Oxyfuel for Cleaner Power Plants

- Coal-burning power plants major source of carbon dioxide emissions
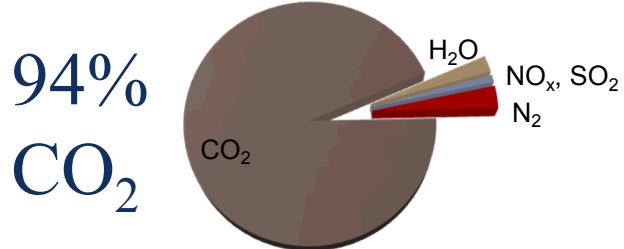
- Interest in capturing CO_2 emissions

What comes out depends on what goes in!

14% CO_2

NO_x, SO

H_2O

CO_2

N_2

Air (78% N_2, 21% O_2)

Stock photo from www.shutterstock.com.

Hu, Y. CO_2 Capture from Oxy-Fuel Combustion Power Plants. Licentiate Thesis, KTH Royal Institute of Technology, Stockholm, Sweden, 2011
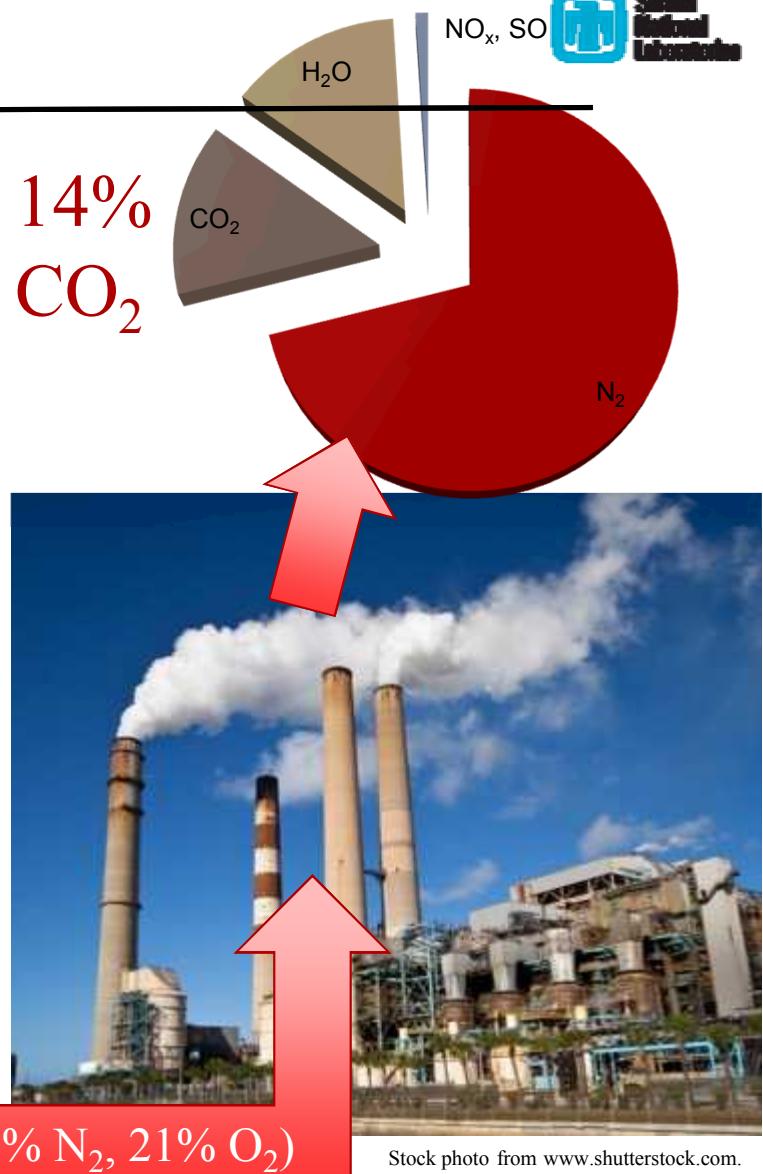
Oxyfuel for Cleaner Power Plants

- Oxyfuel advantages
  - 75% reduction in flue gas volume
  - Decreased NO_x emissions
  - Greater thermal efficiency
  - More energy efficient (not using energy to heat N_2)
  - Easier to capture CO_2

- Goal: MOFs for O_2 separation
  - Alternative to energy-intensive cryogenic separation

94% CO_2

H$_2$O NO$_x$, SO$_2$ N$_2$ CO$_2$

Stock photo from www.shutterstock.com.

Air → MOF → 95% O_2

Hu, Y. CO$_2$ Capture from Oxyfuel Combustion ... Institute of Technology, Stockholm, Sweden, 2011

Integrated Research: Modeling, Materials Development, Combustion Testing, & Techno-economic Analysis

Predictive molecular modeling

Predictive molecular modeling designed to *measure the binding energy for O_2 and N_2* on coordinatively unsaturated metal sites in MOFs
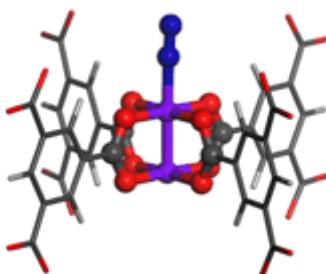
Materials development

Guided by the modeling results, experiments are directed at both the *synthesis of analogs of known/modified materials and of novel frameworks*.
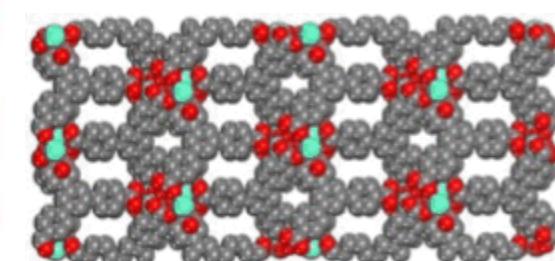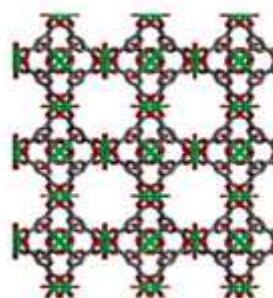
New burner design

New lab burner constructed to mimic practical oxy-fuel combustion in industrial applications: coupling burner design and oxy-fuel combustion to radiant heat transfer
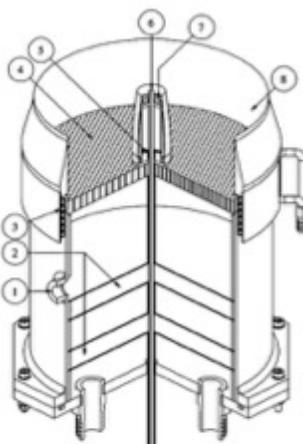
Combust. Flame, 2007, 151, 46

Techno-economic Analysis

Data input to Systems Analysis for calculations of efficiency improvements of combined developed MOFs into Oxy-fuel Process Stream

Input information/data from combustion to systems analysis for calculation of percent efficiency improvements

58

# Is it the framework morphology / channel structure or the choice of metal center?

Initially studied Minimum Energy Binding Modes

O_2 binding to Cr_2(dobdc)
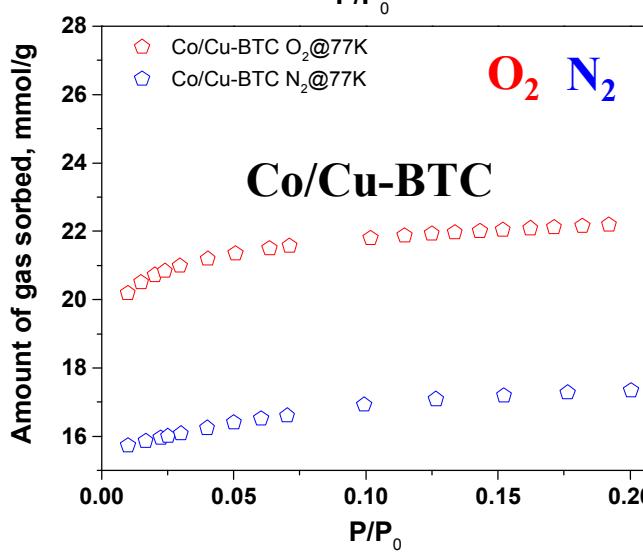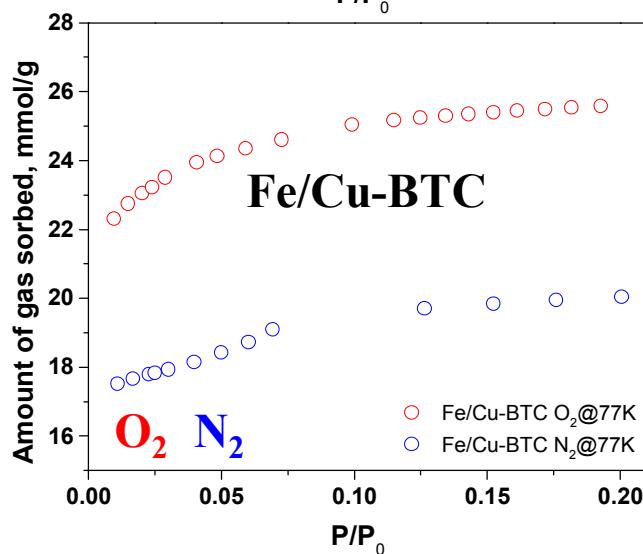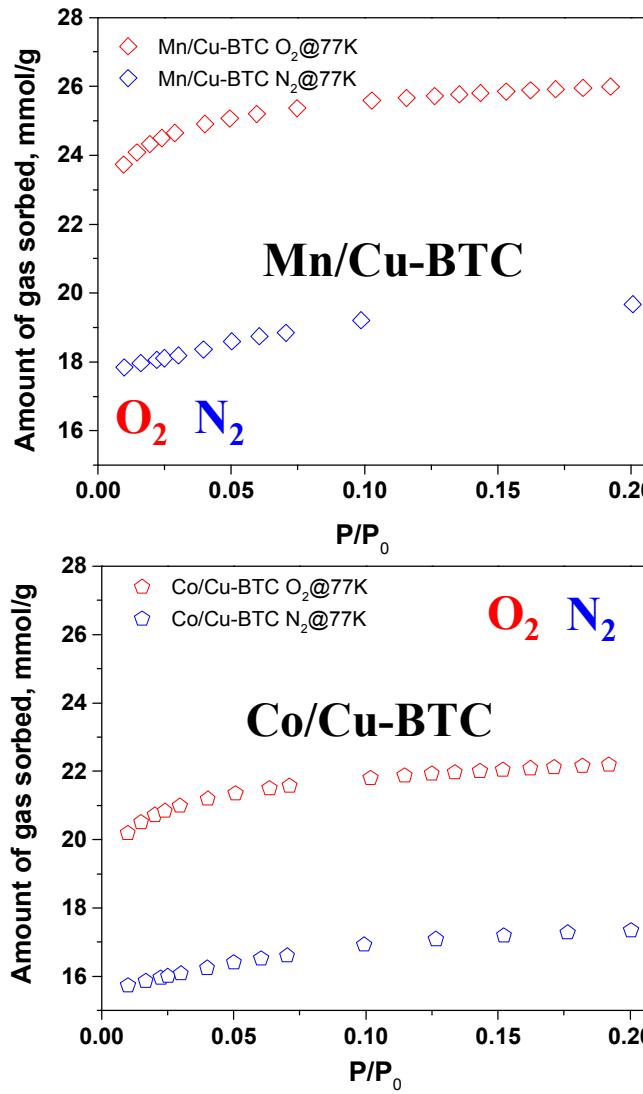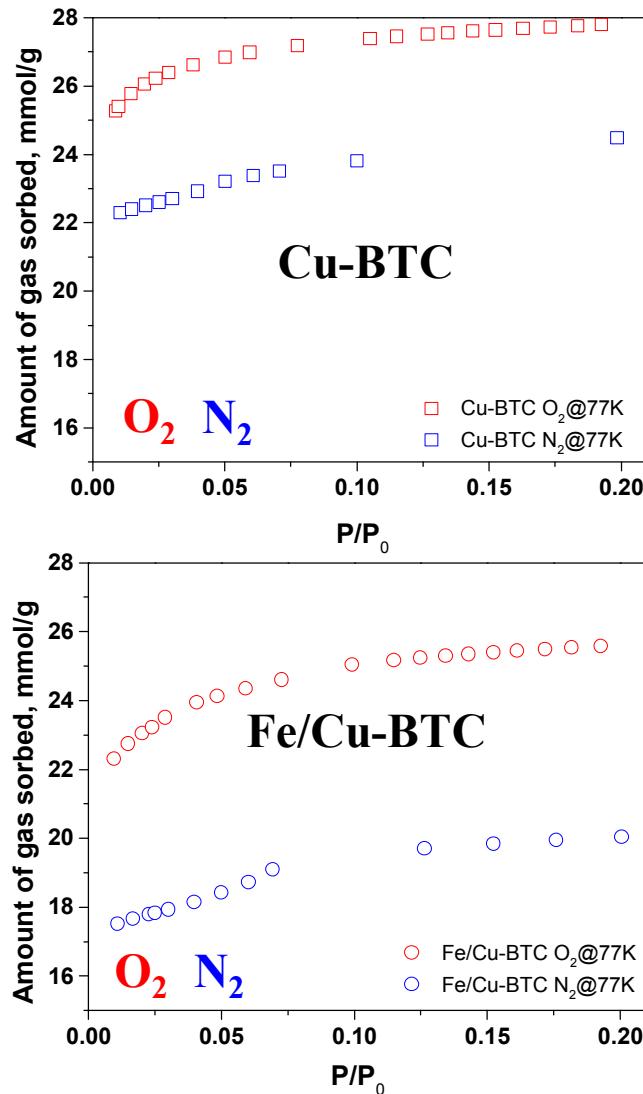
1.4 Å   68°
1.9 Å   1.8 Å
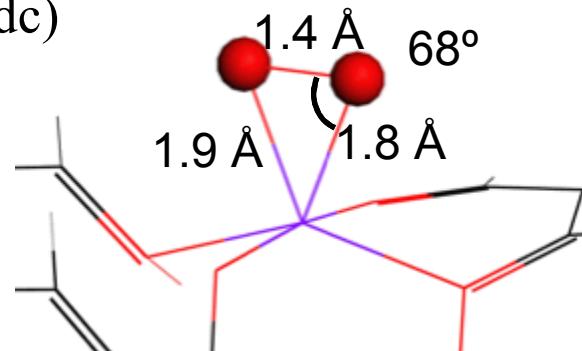
Static

- Side-on bonded, but not showing thermal bent geometry at dynamic binding
- -147 kJ/mol
- *Static configuration*
- *0 K*

Minimum-energy configuration doesn't tell the whole story! "Snap Shot", no thermal effect
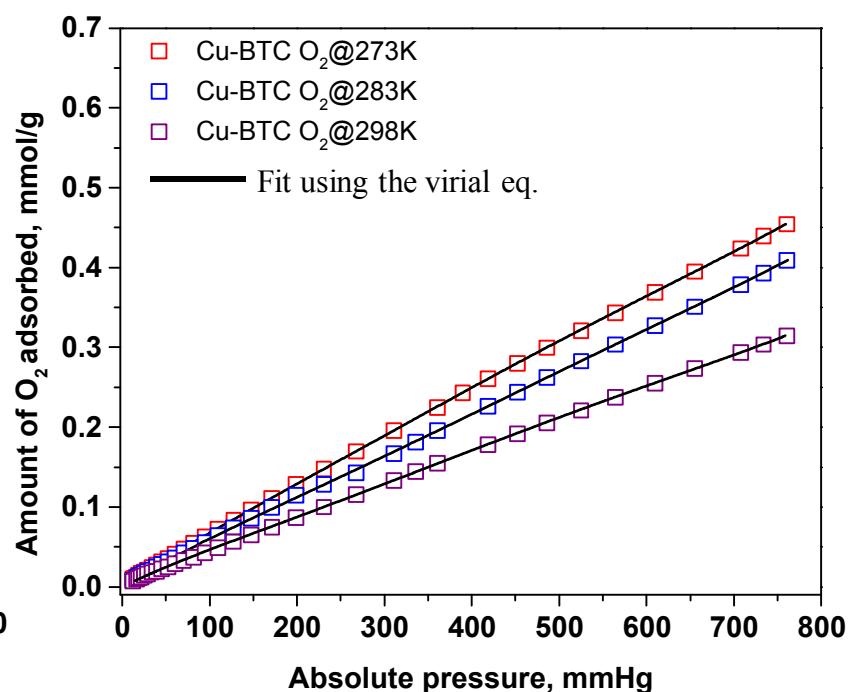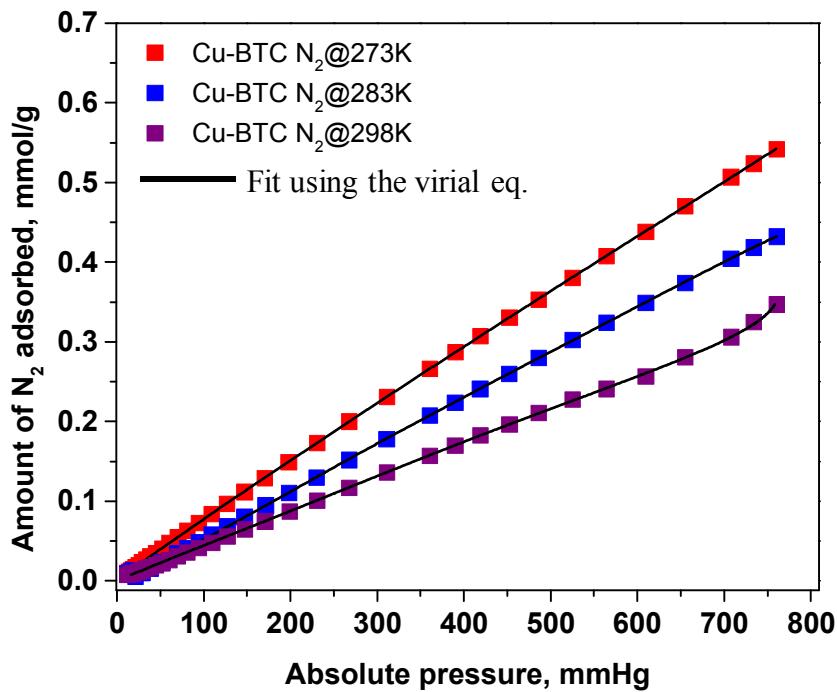
Dynamic
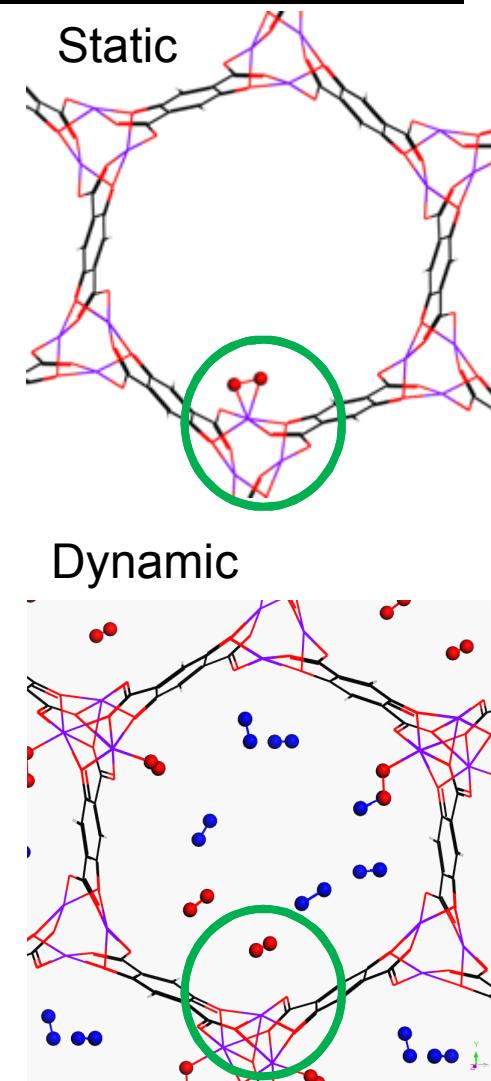
The highest O_2/N_2 selectivity is observed for the Mn/Cu-BTC sample

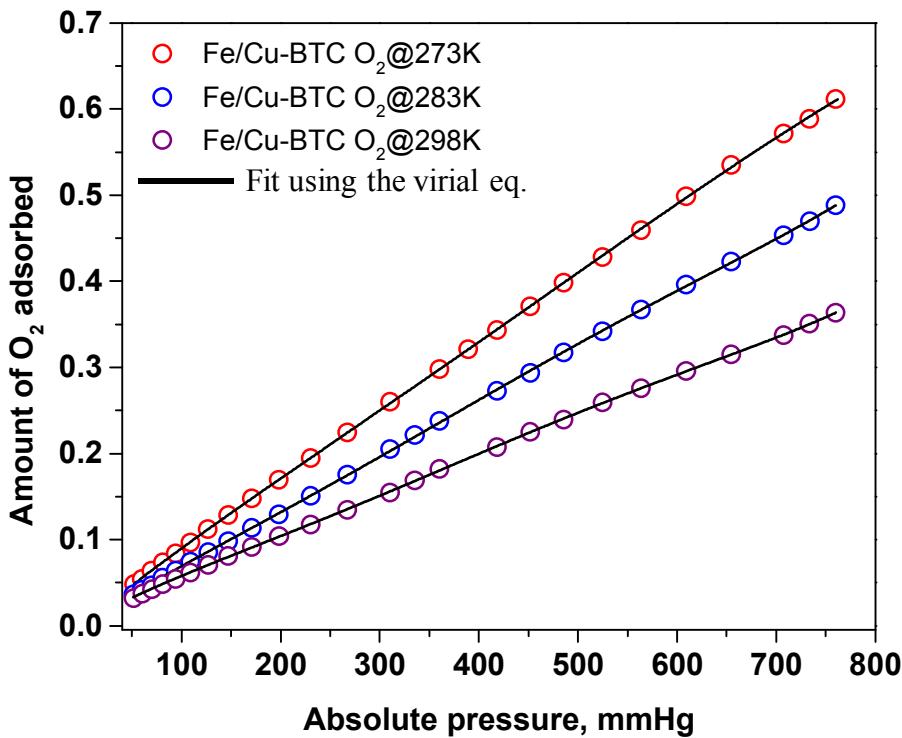# 273-298 K: As Temperature Increases, O$_2$ Loadings Decrease Relative to N$_2$
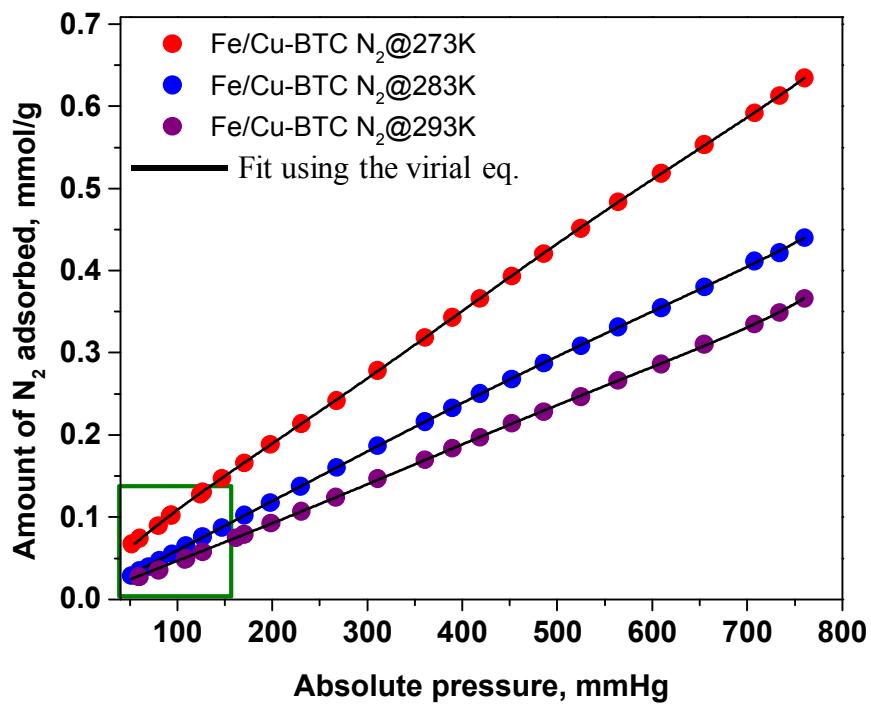
Isotherms in the 273-298K range, *independently* fitted using a modified virial equation:

$$\ln P = \ln N + \frac{1}{T}\sum_{i=0}^{m} a_i N^i$$

Similar behavior noted for the Mn- and Co/Cu-BTC samples

N₂ and O₂ adsorption isotherms measured at 273, 283, and 298K on Fe/Cu-BTC

Similar N₂ and O₂ uptake for Fe/Cu-BTC in the room temperature range

Does it matter which synchrotron?

Yes. Only higher energy storage rings produce significant fluxes of high energy X-rays
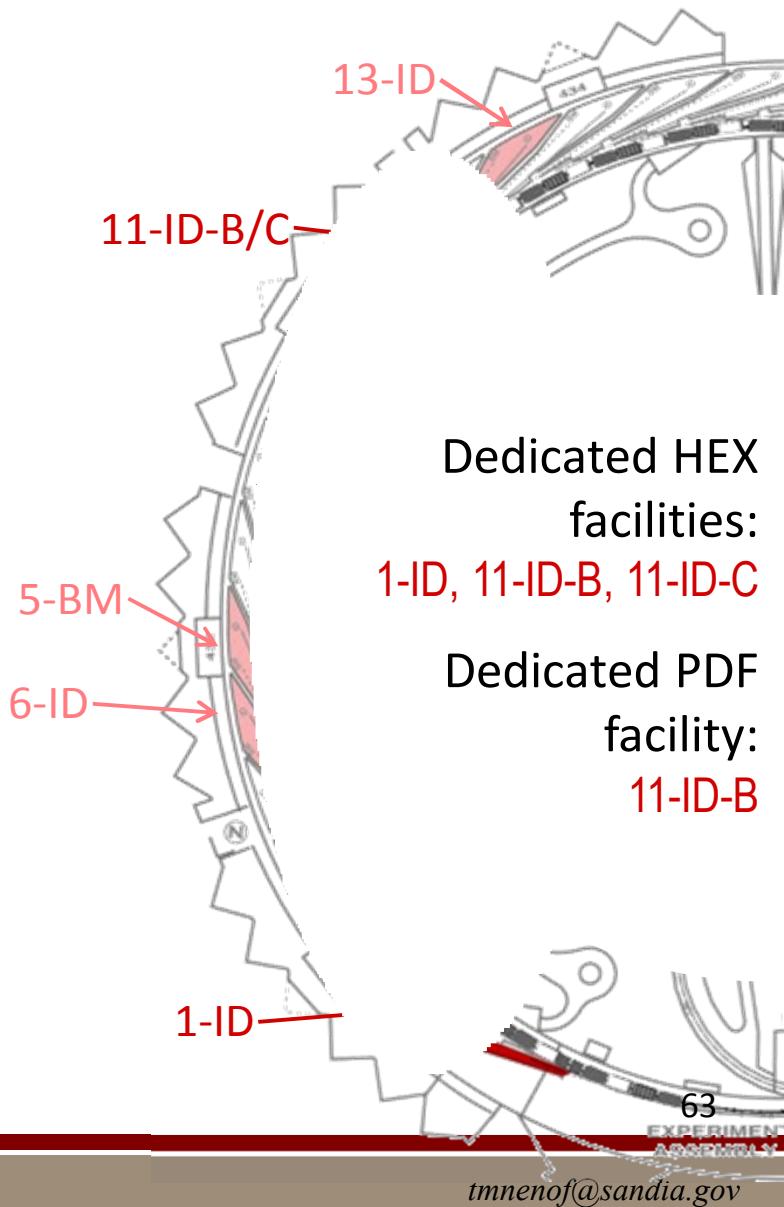
High energy X-rays are a unique strength of the *Advanced Photon Source* (in the western hemisphere)

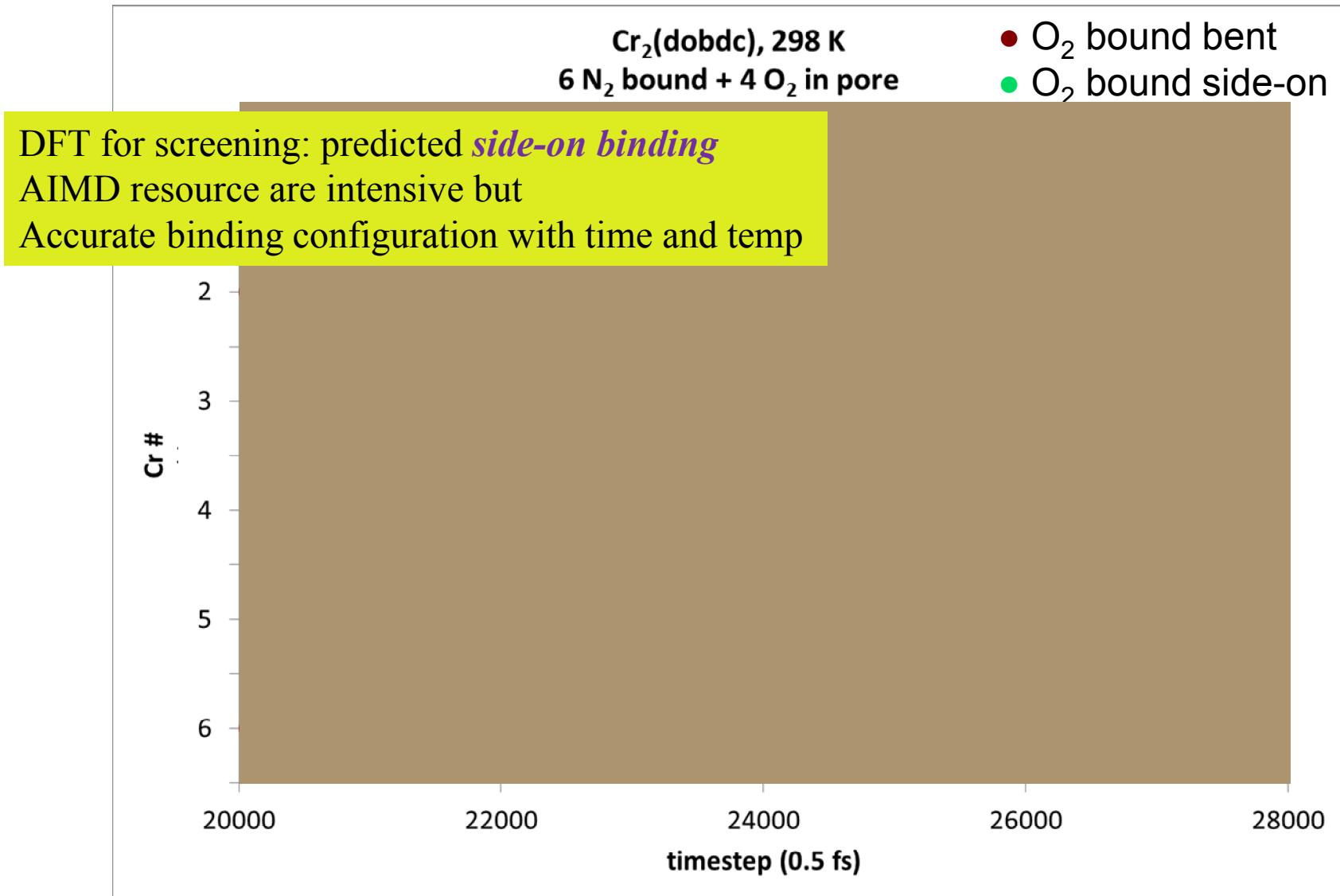- 3 dedicated high energy beam lines
- 1 dedicated PDF beamline

APS 11-ID-B: Dedicated PDF facility
- 58 or 90KeV high energy X-rays
- typical wavelengths = 0.1 - 0.2Å

For our experiments:
$Q > 20$Å^{-1}; CuK$_\alpha$ to $2\Theta = 180$ results in $Q_{max} = 8$Å

13-ID

11-ID-B/C

5-BM

6-ID
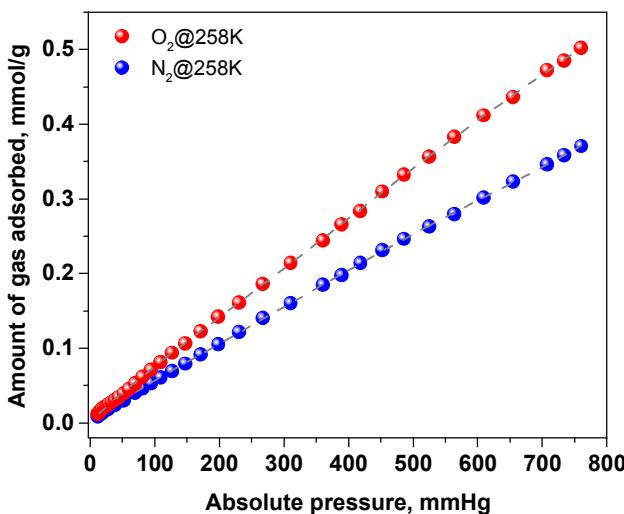
1-ID

Dedicated HEX facilities:
1-ID, 11-ID-B, 11-ID-C

Dedicated PDF facility:
11-ID-B

Cr$_2$(dobdc), 298 K
6 N$_2$ bound + 4 O$_2$ in pore

● O$_2$ bound bent
● O$_2$ bound side-on

DFT for screening: predicted *side-on binding*
AIMD resource are intensive but
Accurate binding configuration with time and temp

Cr #

timestep (0.5 fs)

64

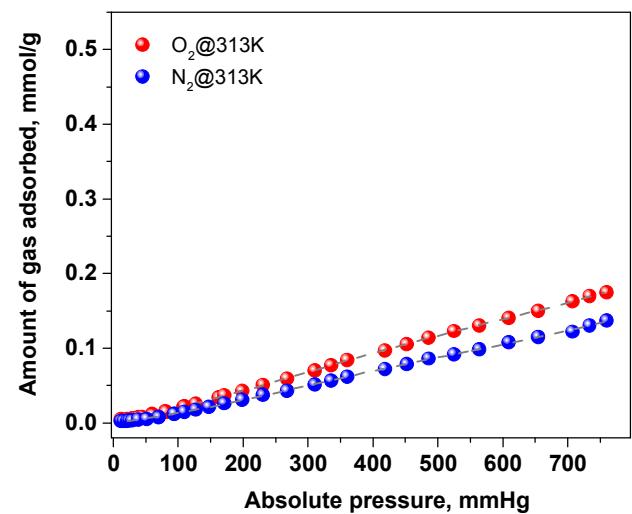Fit using the virial eq.

O_2 vs. N_2 @**258K** O_2 vs. N_2 @**298K** O_2 vs. N_2 @**313K**
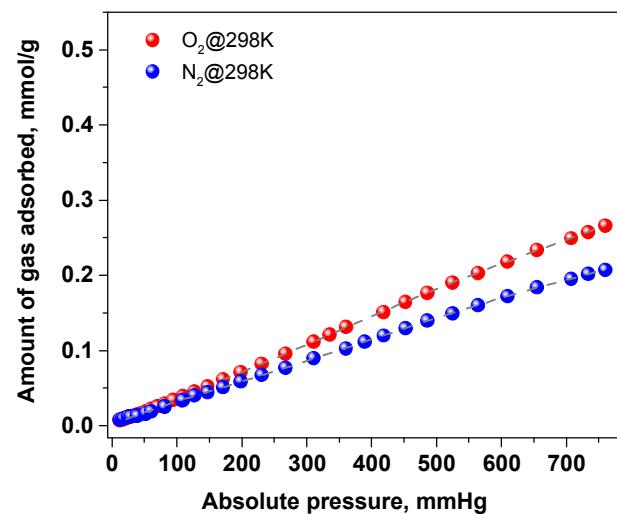
Isotherm trends mimic those predicted by GCMC

Materials Science R&D Objective

We integrate insightful theory, computational simulation tools and experiments to deliver **lifecycle predictivity of materials' performance** *to provide a solid technical basis for engineering decisions. We advance material's design, synthesis, characterization, data analytics, and manufacturing technologies to improve performance and reliability.* **We seek a deep understanding of materials sciences to enable us to resolve issues that arise in materials applications.**